JIMMA UNIVERSITY

COLLEGE OF NATURAL SCIENCE

SCHOOL OF GRADUATE STUDIES

DEPARTMENT OF CHEMISTRY

M.Sc THESIS

ON

SYNTHESIS OF ZnO NANOPARTICLES AND Fe DOPED ZnO NANOCOMPOSITE USING *Zingiber Officinale* ROOT EXTRACT AND EVALUATION OF THEIR ANTIBACTERIAL ACTIVITIES

BY:

YOSEF TAMIRU

ADVISORS: - GUTA GONFA (Ph.D.)

BIRKINESH GIRMA (M.Sc)

JUNE, 2022

JIMMA, ETHIOPIA

SYNTHESIS OF ZnO NANOPARTICLES AND Fe DOPED ZnO NANOCOMPOSITE USING *Zingiber Officinale* ROOT EXTRACT AND EVALUATION OF THEIR ANTIBACTERIAL ACTIVITIES

A RESEARCH THESIS SUBMITTED TO THE SCHOOL OF GRADUATE STUDIES AT JIMMA UNIVERSITY IN PARTIAL FULFILMENT OF THE REQUIREMENTS FOR THE DEGREE OF MASTER OF SCIENCE IN CHEMISTRY

By:

Yosef Tamiru

Approved By:

Advisor:	**Signature**	**Date**
Guta Gonfa (PhD)		_____

_____
Jimma University
College of Natural Sciences
Department of Chemistry

Co-advisor

Birkinesh Girma (M.Sc)		_____

_____
Jimma University
College of Natural Sciences
Department of Chemistry

Internal Examiner

1. **Ahmed Awol** _____

_____

(M.Sc, *Asst. professor of Inorganic Chemistry)*

Jimma University
College of Natural Sciences
Department of Chemistry

ACKNOWLEDGMENT

First of all, I greatly acknowledge Almighty God; I am grateful to my advisor Dr.Guta Gonfa (Ph.D.), and my co-advisor Birkinesh Girma (M.Sc) for their scientific guidance, advice, constructive comments, and continuous support on the topic selection up to the accomplishment of this thesis work. Next, I would like to thank the Material Engineering Department, Institute of Technology, Jimma University for their support in analyzing the FT-IR and XRD of the samples and the Biology department, Jimma University in that they permitted to do antibacterial assay. I would also be thankful to the department of chemistry, at Adama University for conducting SEM analysis for my samples. I have great respect and thanks for Dr. Shimelis for his support during research conducting and Mr.Mulatu (M.Sc) who shared with me his experiences, and valuable information to do well. Finally, I would like to thank the Ministry of Education for allowing me to join this postgraduate program and for sponsorship of my study, my parents, and all the family members who give me moral and material support during my study.

TABLE OF CONTENT

Table of Contents

LIST OF FIGURES

LIST OF TABLES

ABBREVIATIONS

B.cerius	Bacillus cerius
CVD	Chemical vapor deposition
DMSO	Dimethylsulfoxide
$e^- h^+$	Electron hole
E.coli	Escherchia coli
FWHM	Full width at half-maximum
FTIR	Frounter -transmission Infrared
GCE	Glassycarbon electrode
Fe-ZnO NCs	Iron doped Zinc Oxide nanocomposite
Fe-$ZnOs_2$	Iron doped ZnO sample 2
JCPDS	Joint committee powder diffraction standards
Lab.	Laboratory
MHA	Muller-Hinton agar
NI	No inhibition
PE	Plant extract
S.typhi	Salmonella typhi
SEM	Scanning electron Microscopy
S.aurus	Styphlococus aurus
UV	Ultraviolet
XRD	X-ray diffraction
Wt.	Weight
ZnO NPs	Zinc oxide nanoparticles

ABSTRACT

Oxide semiconductors have attracted increasing interest due to their potential in solving environmental problems. The development of antibiotic resistance of bacteria is one of the most pressing problems in world health care. One of the promising ways to overcome microbial resistance to antibiotics is the use of metal oxide nanoparticles and their dopants. This work aims to investigate the synthesis of ZnO NPs and Fe doped ZnO NCs (1%,3%, and 5%) using aqueous *Zingibeer Officianale* root extract via biosynthesis and evaluation of its antibacterial activities. The synthesized nanoparticles and nanocomposites were characterized using X-ray diffraction (XRD), UV-Vis spectrophotometer, Fourier transform infrared spectroscopy (FTIR), and Scanning Electron Microscopy (SEM). The optical band gaps were calculated to be Eg = 3.12 eV and Eg = 3.0 eV for ZnO NPs and 1% Fe doped ZnO NCs respectively. Functional groups present in the extract, NPs, and NCs were confirmed by FTIR spectroscopy. The average particle size calculated from the XRD pattern for ZnO NPs and Fe doped ZnO nanocomposite were 23 and 19.6 nm respectively. SEM analysis showed that ZnO nanoparticles were a granular size and has irregular spherical morphology while with Fe doped ZnO nanocomposite there is dispersion with less agglomeration as well as regular distribution of ZnO NPs. The synthesized NPs and NCs were tested for their antibacterial properties on two Gram-negative bacteria: Escherichia coli (E.coli) and Salmonella typhi (S.typhi) and two Gram-positive bacteria: Bacillus cerius (B.cerius) and Staphylococcus aureus (S.aurus). The results showed that ZnO NPs have an antibacterial inhibition zone of 10 mm and 14 mm against E. coli and S. aureus, and 15 mm and 9 mm against B. cereus and S. typhi respectively at a concentration of 50 mg/mL. Those synthesized NPs and NCs were more effective on Gram-negative bacteria than gram-positive. Thus, the bactericidal activity of Fe doped ZnO NCs was more prominent with S. aureus and B. cerius than S.typhi and E. coli bacteria and when compared to ZnO NPs.

Keywords: Fe doped ZnO Nanocomposites, *Zingiber Officinale*, Gram-Negative Bacteria, Antibacterial Activities, Green synthesis.

1. INTRODUCTION

1.1. Background of the study

Many Physico-chemical methods have been used so far to synthesize nanoparticles that are tedious and possess hazardous solvents or reagents as the expensive substrate with potentially adverse effects, as well as requiring specific instrumentation [1,2]. Synthesis of nanoparticles via eco-friendly, i.e. green synthesis, provides simplicity, low cost, ambient atmosphere synthesis, non-toxicity, and environmental compatibility [3, 4]. Due to these novel properties, green synthesis has attracted various researchers in the scientific community from around the world. Green synthesis of metal nanoparticles is an exciting subject of nanoscience as it provides the most stable nanoparticles with varying shapes [5]. Plant extracts have been found an up-and-coming candidate for facile synthesis of nanoparticles. Zinc Oxide (ZnO) is an essential inorganic semiconductor material due to its high photostability, nontoxicity, thermal stability, oxidation resistivity, and high electron mobility [6,7]. The biological applications of ZnO nanoparticles make them ideal candidates for biological sensing, gene delivery, drug delivery, wound dressing material, antifungal, and antibacterial activities [8-10]. Besides, ZnO nanoparticles are inexpensive and exhibit morphological versatility such as nanorods, nanoflowers, nanospheres, nanotubes, etc., and were more influential on rheological parameters [11-14]. Photocatalytic processes driven by ZnO nanostructure semiconductors have great potential for decontamination of organic compounds in water due to ease, complete mineralization of pollutants, and being environmentally friendly [15]. Semiconductor photocatalysts have recently demonstrated high photocatalytic activity for decontamination and Iron oxide nanoparticles combined with semiconductor, which promotes the separation of charges, produces more photo-generated charges [16, 17]. Heterogeneous hybrid systems also have developed as compelling. In this work, the structural and anti-microbial activity of ZnO and Fe doped-ZnO NCs prepared via a green synthesis approach have been taken into consideration.

Among the transition metals, iron (Fe) is preferred for doping of ZnO due to easily overlapping of its *d*-electrons with the ZnO valance band. It has also been reported that Fe-doped ZnO nanoparticles can enhance antibacterial and magnetic properties. Numerous methods have been applied for the transition metal-doped ZnO nanoparticles [18-19]. ZnO NPs are one of the n-type

semiconductors and the most extensively used materials in a variety of applications [20]. However, ZnO NPs are considered extremely toxic to the environment, and their wide band gap (Eg =3.37 eV) has created limited practical applications as photocatalyst and antimicrobial agents [21]. The enhancement of its photocatalytic activity in the visible region and the reduction of ZnO toxicity can be achieved by NP doping strategies[22]. Some transition metal ions, e.g., Co^{2+}, Mn^{2+}, Ti^{4+}, La^{3+}, and Fe^{3+}, have been doped into ZnO. The transition metal-doped ZnO NPs show better traits such as narrow or split band gap, enhanced interfacial charge transfer rate, and antibacterial activity [23]. In particular, Fe-ZnO has been frequently explored for biomedical applications such as dye degradation reagents, toxic dye absorbers, wound treatment, cancer treatment, drug delivery, etc. due to its high antimicrobial activities [24]. ZnO nanoparticles have many significant features of chemical and physical stability, high catalysis activity, and effective antibacterial activity [25-29].

Various techniques have been employed to synthesize ZnO nanoparticles, including sol-gel method, vapor deposition, precipitation, thermal decomposition, hydrothermal synthesis, and spray pyrolysis [30-31]. Among the various known synthesis methods, plant-mediated nanoparticle synthesis is preferred since it is cost-effective, environmentally friendly, and safe for human therapeutic use and a single-step method for the biosynthesis process [32]. Biological methods of nanoparticle synthesis using microorganisms, enzymes, and plant extracts have been suggested as possible eco-friendly alternatives to chemical and physical methods [33]. Biosynthesized nanoparticles are now known for their use in biosensors, water purification processes, catalyst, antibacterial, antiviral, and anti-insect-like applications [34]. The main active plant-based multifunctional agents are polyphenols and flavonoids that have strong roles in the synthesis and stabilization of metal NPs [35]. In recent years, inorganic antimicrobial agents are being increasingly used for the control of microorganisms in various areas [36]. The considerable antimicrobial activity of inorganic metal oxide NPs, such as ZnO, MgO, TiO_2, and SiO_2, and their selective toxicity in biological systems suggest that the potential application in therapeutics, diagnostics, surgical devices, and nanomedicine. Green synthesis of zinc oxide (ZnO) nanoparticles using different plant extracts of Azadirachta indica, Hibiscus rosa-sinensis, Murraya koenigii, Moringa oleifera, and Tamarindus indica for biological applications has been reported [37]. Ginger (*Zingiber officinale* Roscoe, Zingiberaceae) is among the most frequently

and heavily consumed dietary condiments throughout the world. Ginger is frequently prescribed by Indian and Chinese medicine for the treatment of cough, common cold, rheumatism, snake bite, and respiratory problems. It is also used in the treatment of colorectal cancer, treating skin diseases, cough, heart palpitation, swelling, dyspepsia, and loss of appetite [38]. Chemically, ginger is rich in flavonoids and polyphenolic compounds such as gingerols, shagols, zingerone, paradol, terphineol, terpenes, borneol, geraniol, limonene, linalool, alpha zingiberene, etc. Recent studies that revealed that ginger can be used for the synthesis of nanoparticles have reported that an aqueous extract of ginger was used for the synthesis of gold and silver nanoparticles [39-40]. The main objective of the present investigation focused on the synthesis of ZnO NPs and Iron doped ZnO NCs from zingiber *officinale* root extract and the evaluation of its antibacterial activity.

1.2. The statement of the problem

The conventional methods of nanoparticle synthesis, via physical and chemical methods, have been remaining expensive, use toxic, hazardous, and non-eco-friendly chemicals, use high pressure, temperature, and energy, and required complicated operative conditions. Therefore the great need for a cost-effective and eco-friendly method attracted the attention of researchers to develop biological methods using plant extracts. Resistance of microbial to antibiotics has increased in recent years. Some antibacterial agents are extremely irritant and toxic and there is much interest in finding a way to formulate a new type of safe and cost-effective biocidial materials. Metallic/oxide nanoparticles and nanocomposites are thoroughly being explored and extensively investigated as potential antibacterial. Many plant extract-mediated synthesis of ZnO nanoparticles and their wide application as an antibacterial agent have been reported in the various literature [38]. However, the synthesis of ZnO nanoparticles and Fe doped ZnO nanocomposite using *zingiber officinale* rhizome extract has not been reported so far. Therefore this study focused on *zingiber officinale* rhizome extract mediated synthesis of ZnO nanoparticle and Fe doped ZnO nanocomposite and evaluation of its antibacterial activity.

Generally, this research was designed to answer the following questions:

- Is the selected plant extract rich in secondary metabolites which responsible for ZnO NPs and Fe-ZnO NCs synthesis?

- Does the applications of the synthesized Fe-ZnO NCs consistent with the reported values in related works of literature?
- Is the application useful for society in controlling biocidals?

1.3. Objectives

1.3.1. General objective

- To synthesize ZnO nanoparticles and Fe doped ZnO nanocomposite using *zingiber officinale* rhizome and evaluation of its antibacterial activities.

1.3.2. Specific objectives

- To prepare ginger (*zingiber officinale*) rhizome extract supported ZnO nanoparticles and their Fe doped ZnO nanocomposites.
- To characterize the synthesized ZnO NPs and Fe doped ZnO nanocomposites using techniques: UV-Vis spectroscopy, FT-IR, SEM, and XRD.
- To evaluate the antibacterial activity of the synthesized ZnO NPs and Fe doped NCs.

1.4. Significance of the study

In recent years, there is an increasing demand for Synthesizing of ZnO NPs and Fe doped ZnO NCs due to their wide application. Thus, the most effective, cheap, and simplest technique of nanoparticle synthesis becomes a much more interesting area of research. Therefore, the development of biological methods of synthesis using plant extract is an essential method.

In general, the findings of this study have the following significance.

- Providing further awareness for researchers about antibacterial applications of green synthesized ZnO NPs and Fe doped ZnO NCs.
- This study provided baseline information for other researchers who want to work in this area
- Upgrading the knowledge about the Fe doped ZnO NCs regarding its antibacterial activity.

2. REVIEW LITERATURE

2.1. Nanomaterial's:

Nanomaterials are cornerstones of nanoscience and nanotechnology. It has the potential for revolutionizing how materials and products are created and the range and nature of functionalities that can be accessed. It is already having a significant commercial impact, which will assuredly increase in the future [39]. Nanoscale materials are defined as a set of substances where at least one dimension is less than approximately 100 nm. A nanometer is one-millionth of a millimeter- approximately 100,000 times smaller than the diameter of a human hair. Nanomaterials are interesting because at this scale unique optical, magnetic, electrical, and other properties emerged [40]. These emergent properties have the potential for great impacts in electronics, medicine, and other fields.

2.1.1. Classification of nanomaterials:

Nanomaterials have an extremely small size having at least one dimension of 100 nm or less. They can be nanoscale in one dimension (eg. surface films), two dimensions (eg. strands or fibers), or three dimensions (eg. particles). They can exist in single, fused, aggregated, or agglomerated forms with spherical, tubular, and irregular shapes. Common types of nanomaterials include nanotubes, dendrimers, quantum dots, and fullerenes [41]. Nanomaterials have applications in the field of nanotechnology and display different physical-chemical characteristics from normal chemicals (i.e., silver nano, carbon nanotube, fullerene, photocatalyst, carbon nano, and silica). According to Siegel, Nanostructured materials are classified as Zero dimensional, one dimensional, two dimensional, or three-dimensional nanostructures [42].

2.1.2. Nanomaterial synthesis and processing

We are dealing with very fine structures: a nanometer is a billionth of a meter. This indeed allows us to think in both the 'bottom up' or the 'top down' approaches to synthesize nanomaterials, i.e. either to assemble atoms or to dis-assemble (break, or dissociate) bulk solids into finer pieces until they are constituted of only a few atoms. This domain is a pure example of interdisciplinary work encompassing physics, chemistry, and engineering up to medicine [43].

2.1.2.1. Wet Chemical Synthesis of Nanomaterials

In this principle we can classify the wet chemical synthesis of nanomaterials into two broad groups:

1. **The top-down method:** where single crystals are etched in an aqueous solution for producing nanomaterials, For example, the synthesis of porous silicon by electrochemical etching.

2**. The bottom-up method**: consists of sol-gel method, precipitation, etc. where materials containing the desired precursors are mixed in a controlled fashion to form a colloidal solution.

2.1.2.1.1. Sol-gel process

The sol-gel process involves the evolution of inorganic networks through the formation of a colloidal suspension (sol) and gelation of the sol to form a network in a continuous liquid phase (gel). The precursors for synthesizing these colloids consist usually of a metal or metalloid element surrounded by various reactive ligands. The starting material is processed to form a dispersible oxide and forms a sol in contact with water or dilute acid. Removal of the liquid from the sol yields the gel, and the sol/gel transition controls the particle size and shape. Calcination of the gel produces the oxide [44]. Sol-gel processing refers to the hydrolysis and condensation of alkoxide-based precursors such as Si $(OEt)_4$ (tetraethyl orthosilicate, or TEOS). Sol-gel method of synthesizing nanomaterial is very popular amongst chemists and is widely employed to prepare oxide materials. The sol-gel process can be characterized by a series of distinct steps [45].

2.1.2.2. Gas Phase synthesis of nanomaterials:

The gas-phase synthesis methods are of increasing interest because they allow an elegant way to control process parameters to be able to produce size, shape, and chemical composition controlled nanostructures. Before we discuss a few selected pathways for the gas-phase formation of nanomaterials, some general aspects of gas-phase synthesis need to be discussed. In conventional chemical vapor deposition (CVD) synthesis, gaseous products either are allowed to react homogeneously or heterogeneously depending on a particular application [46].

2.2 Doping

Doping of transition metals, noble metals, or lanthanide ions is the method employed for retarding the fast charge recombination and enabling visible light absorption by creating defect states in the band gap.

2.2.1 Metal doped ZnO NPs

Metal doping of ZnO can improve the antimicrobial activity of catalysts by increasing the trapping site of the induced charge carriers and thus decreasing the recombination rate of induced electron-hole pairs [47]. To decrease the band gap energy of photo-catalysts, metal dopants such as Ce, Nd, Cu, and Al have been used in applications in dye degradation and gas sensors [48]. They have shown that higher loads of organic compounds could be adsorbed on Al-doped ZnO compared to ZnO NPs based on the high light harvesting efficiency [49]. It is also reported that the incorporation of metal ions such as Fe^{3+}, can contribute to more oxygen defects on ZnO along with an increase in the charge density of ZnO, which subsequently can induce higher performance of the nanostructure.

2.2.2. Non-metal doped ZnO NPs

In the nonmetal doping case, the incorporation of dopant leads to the creation of local states inside the band gap and the absorption on a set of semiconductors can be extended from the UV to the visible-light region through band gap narrowing [50]. ZnO doping with nonmetals, such as carbon (C), nitrogen (N), and sulfur (S) can lead to the formation of intermediate energy levels and extend the valence band, which causes visible light photocatalytic activity. Shelja [51] synthesized N-ZnO/C-dots nanoflowers for Mg Methyl blue degradation under visible light irradiation. The photocatalytic efficiency of N-ZnO/C is (85%) which is higher than ZnO (65%). Hanggara [52] reported the synthesis of visible light active N doped ZnO through a combustion reaction. The N doped ZnO show 89.3% of MB degradation with an initial concentration of 10 mg/L within1.5 hrs under visible light. Weilai [53] also studied C, N, and S doped ZnO and investigated the electronic structures, optical properties, and effective masses of charge carriers by first-principle density functional theory calculation. The calculation of the effective masses shows that ZnO typically possesses light electrons and heavy holes, confirming its intrinsic character as an n-type semiconductor, while N, C and S doping can generally render electrons

lighter and holes heavier, resulting in a slower recombination rate of photogenerated electron-hole pairs.

2.3. Botanical Description of *zingiber officinale* plant

2.3.1. Plant description

Ginger is a 2-4 foot tall perennial with grass-like leaves up to a foot in length. It is the underground root or rhizome that is used for culinary and medicinal purposes. Ginger root is the rhizome of the *zingiber officinale* plant and it is a slender herbaceous perennial herb. Ginger is cultivated in the tropics and it requires a warm and humid climate flourishing in well-drained friable soil, though it can also be grown in a light soil rich in humus. Ginger is the underground rhizome of the ginger plant with a firm striated texture. The flesh of the ginger rhizome can be yellow, white, or red depending upon the variety [61]. It is covered with brownish skin that may either be thick or thin and it is consumed as a delicacy, medicine, or spice. The characteristics of odor and flavor of ginger are caused by a mixture of zingerone, shogaol, and gingerol. Ginger produces clusters of white and pink flower buds that bloom into a yellow flower and due to its aesthetic appeal and the adaption of the plant to warm climates, ginger is often used as landscaping around subtropical homes [62-63].

2.3.2 .Vernacular names

Table 1: Name of *zingiber officinale* that are given by some different countries and languages [64-65].

No	Countries(Language)	Name of *zingiber officinale*
1	Arabic	*Zanjabal*
2	China	*Gan-Jiang*(dried) ,sheng *jiang* (fresh)
3	Dutch	*Gember*
4	English	*Ginger*
5	French	*Gingembre*
6	German	*Ingwer*
7	Spanish	*Jengibre*
8	Sanskrit	*Adraka* (fresh)
9	Shunthi	*Shringaveran*

10	Japan	*Shouga*
11	Amharic	*Zinjibl*
12	Afan Oromo	*Zinjibal*
13	Urdu and Hindi	*Adrak* (fresh) , *Sonth* (dry)

2.3.3. Scientific classification of Ginger:

Division: Magnoliophyta; Class: Liliopsida ; Order: Zingiberales ; Family: Zingiberaceae

Genus: Zingiber; Species: *Zingiber Officinale*

2.3.4. Medicinal values and Phytochemistry of ginger

Medicinal plants with recognized therapeutic features and no side effects have attracted much attention. *Zingiber officinale* Roscoe (ginger) is among these plants. It belongs to the family Zingiberaceae and has been traditionally consumed as a spice with strong therapeutic activity [66]. Ginger has been widely used in ethnomedicine for the cure of several ailments. In modern Phytotherapy, ginger preparations are predominantly used to counteract nausea and vomiting in pregnant women but they have anti-inflammatory, analgesic, and metabolic actions in clinical applications in knee osteoarthritis, dysmenorrhea, type-2 diabetes, hyperlipidemia, overweight, and obesity [67]. There are more than 400 different compounds in ginger which include carbohydrates, lipids, terpenes, zingiberene,

β-bisabolene, α-farnesene, β-sesquiphellandrene, α-curcumin, gingerols, paradols, and shogaols . Given that, ginger is plentiful in antioxidants, and the biomolecules in the ginger extract are assumed to play a critical role in the reduction of metal ions to metallic NPs]. The anti-inflammatory properties of ginger have been known and valued for centuries. This contains many phytochemicals such as alkaloids, saponins, tannins, and flavonoids. (It includes Pantothenic acid, Vit B6, Folate, Vit C, Calcium, Iron, Magnesium, and Manganese). To the best of our knowledge, a biological approach using powder extract of dry ginger rhizome has been used for the first time as a reducing material as well as a surface stabilizing agent for the synthesis of spherical ZnO [68-70]. Many Metal and non-metal Nanoparticles and nanocomposite Research are conducted plant-mediated. Some of the recent reports on the plant-mediated synthesis of ZnO NPs and Fe-ZnO NPs summarized as follows:

Table 2: The Recent study conducted by a different types of plants to synthesize ZnO Nanoparticles and Fe-ZnO Nanocomposite

No	Plants	Part Used	Nanopart icle	Size(nm)	studies	Reference
1	Alotropis gigintean	Leaves	ZnO	30-35	Characterization	[71]
2	Aloe Vera	Leaves	ZnO	40	Antimicrobial	[72]
3	Ixora coccinea	Leaves	ZnO	32-51	catalytic	[73]
4	Acalypta indica	Leaves	ZnO	45	Characterization	[74]
5	Seaweeds	whole	ZnO	36	Characterization	[75]
6	Cassia auriculata	flower	ZnO	80-90	Characterization	[76]
7	Salvadora persica	Leaf	ZnO	30-50	Catalytic	[77]
8	Allium sativum	Bulbs	ZnO	47.57	synthesis	[78]
9	Parthenium hysterophorus	Leaf	ZnO	16-45	Antimicrobial	[79]
10	Vitis vinifera	Leaf	ZnO-Ag		Antimicrobial	[80]
12	V.trifolia	Leaf	ZnO		Antimicrobial	[82]
13	Emblica Officinalis	fruit	ZnO		Antimicrobial	[83]
14	Carica papaya	Leaf and stem bark	ZnO		Antimicrobial	[84]
16	Zingiber officinale	Root	ZnO		Antimicrobial	[86]

Phenolic compounds of Ginger[88]

Gingerol Gallic acid Shagoal

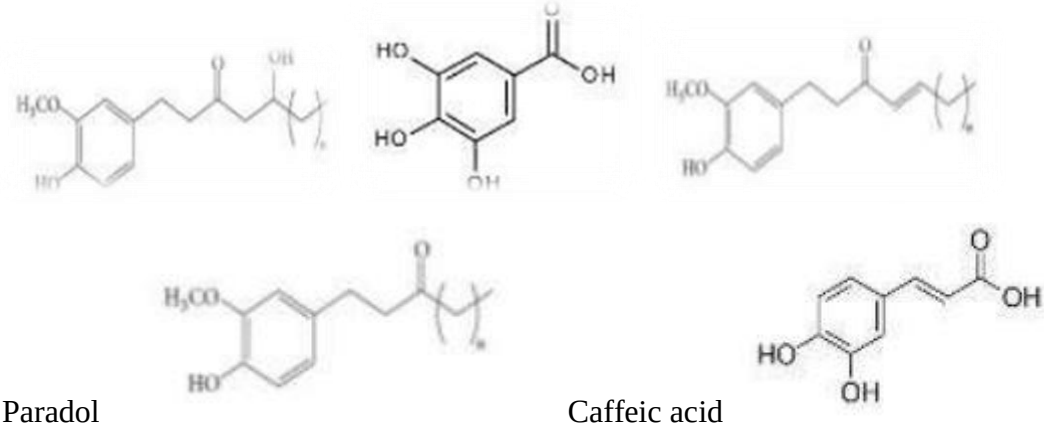

Paradol Caffeic acid

Catechin chlorogenic acid Protochatecuitic

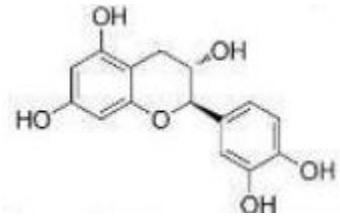

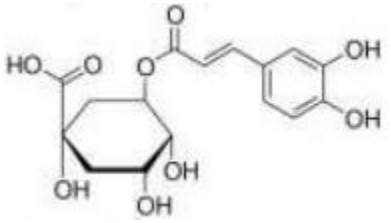

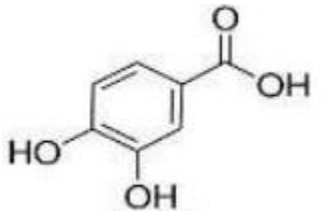

Flavonoids compounds of ginger

Luteolin Rutin Rosmarinic acid

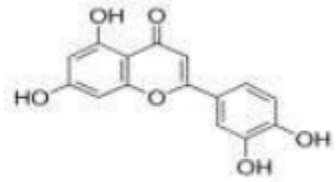

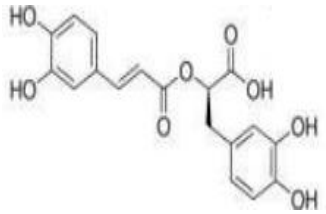

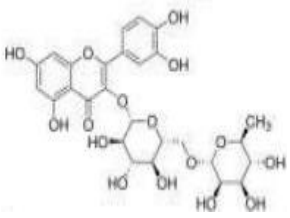

2.4. Green Synthesis of ZnO nanoparticles

Among the metal oxide nanoparticles, zinc oxide is interesting because it has vast applications in various areas such as optical, piezoelectric, magnetic, and gas sensing. Besides these properties, ZnO nanostructure exhibits high catalytic efficiency, and strong adsorption and is used frequently in the manufacture of sunscreens [54], ceramics, and rubber processing, wastewater treatment, and as a fungicide. ZnO has large excitation binding energy (60 m eV) which allows UV lasing action to occur even at room temperature and ZnO with Oxygen vacancies exhibits an efficient green emission. Several physical and chemical procedures have been used for the synthesis of large quantities of metal nanoparticles in a relatively short period. But chemical methods lead to the presence of some toxic chemicals adsorbed on the surface that may have

adverse effects in medical applications. Currently, plant-mediated Biological synthesis of nanoparticles is gaining importance due to its simplicity, eco-friendliness, and extensive antimicrobial activity [56]. Biosynthesis of zinc oxide nanoparticles by plant *zingiber officinale* has been reported.

The plant ginger belongs to the family of *Zingeiberaceae* and is a common condiment for various foods and beverages. It has an ailing history of medicinal use in India for conditions such as headaches, nausea, rheumatism, and colds. The structure, phase, and morphology of the synthesized product were investigated by the standard characterization techniques [57]. Synthesis of zinc oxide nanoparticles can be performed using many routinely used chemical and physical methods [59]. However, the green synthesis of zinc oxide nanoparticles is an interesting issue in nanoscience and nanobiotechnology. Nanoparticles produced by plants are more stable, and the rate of synthesis is faster. Moreover, the nanoparticles are more varied in shape and size in comparison with those produced by other methods [60].

2.5. Antibacterial activity of Fe doped ZnO nanoparticles

Zinc Oxide (ZnO) is an essential inorganic semiconductor material due to its high photostability, nontoxicity, thermal stability, oxidation resistivity, and high electron mobility. ZnO nanoparticles, in particular, are environment-friendly, offer easy fabrication, and are non-toxic, bio-safe, and biocompatible [88]. The biological applications of ZnO nanoparticles make them ideal candidates for biological sensing, gene delivery, drug delivery, wound dressing material, antifungal, and antibacterial activities [89]. The organic components played an important role in the morphology and texture of the final products [90]. The conventional methods used toxic chemicals and non-polar solvents as synthetic additives or capping agents [91]. Simple and biocompatible processes are needed for the inexpensive synthesis of non-toxic NPs. In the biological methods, bacteria, fungi, actinomycetes, yeasts, and plants have been used as reducing agents for the synthesis of various NPs [92]. Akhtar et al. have reported that the biogenic synthesis of NPs from plant extract seems to be an effective method in raising facile, innocuous, and biocompatible NPs [93]. The inhibition zones were measured by taking the nanostructure solution. Ampicillin showed the appearance of inhibition zones of different sizes in different bacteria and Fluconazole showed an inhibition zone against *C.* Albicans [94-95]. The presence of

a zone of inhibition demonstrates the mechanism of the activities of ZnO nanoparticles, which includes interruption of the membrane with a high rate of multiplication of surface oxygen species and at last go to the death of pathogens [96-97]. Interestingly, the size of the inhibition zone was different according to the type of pathogens, synthesis method, and the concentrations of nanoparticles [98-99].

Mechanism of Antibacterial activity

The concentration of ZnO NPs when extended the zone inhibition diameter range (mm) can also be extended to increased H_2O_2 concentration on ZnO NPs surface. The mechanisms of antimicrobial activities of ZnO NPs, (Fig.) most of the defects can be activated by both UV and visible light; as a result, electron-hole pairs (e^- h^+) can be created. The holes split H_2O molecules from ZnO into OH^- and H^+. Dissolve oxygen molecules are transformed into superoxide radical anions (O_2), which in turn react with H^+ to generate (H_2O_2) radicals, which upon successive collision with electrons create hydrogen peroxide anions (H_2O_2). Then they react with hydrogen ions to generate molecules H_2O_2. The generated H_2O_2 molecules can penetrate the cell membrane and kill the bacteria [112].

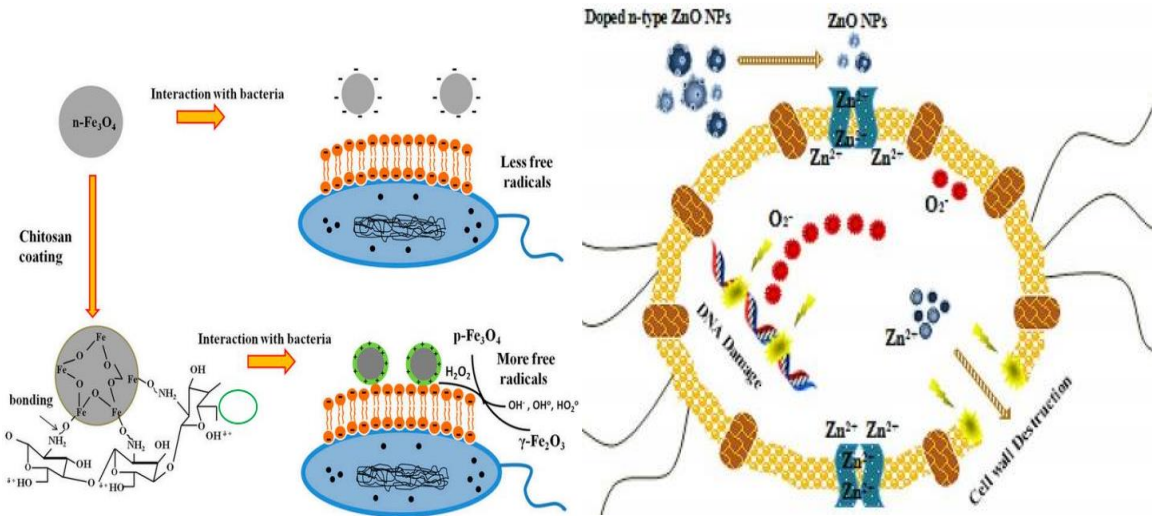

Figure 1: Antibacterial activity of ZnO NPs and Fe oxide NPs

3. MATERIALS AND METHODS

3.1. Chemicals, Materials, and Reagents

All the chemicals and reagents used in this study were of analytical grade: Zinc nitrate hexahydrate ($Zn(NO_3)_2.6H_2O$) (Himedia), Ferric Chloride ($FeCl_3$) (Himedia), and, 2M of sodium hydroxide NaOH, Ethanol,(CH_3CH_2OH), Distilled water and dilute Hydrochloric acid (HCl). *Zingiber officianale* Plant root extract

3.2. Instruments and apparatuses

3.2.1. Apparatuses

Centrifuge, Oven, Mortar and pestle, Digital Balance, Hot plate, Magnetic stirrer, Watch, Filter paper, funnel, Beakers, Test tubes, Droppers, Graduated cylinders, Glass rod, Erlenmeyer flask, cuvettes, PH meter, spatula,

3.2.2. Instruments

Double beam Uv-vis spectrophotometer (C/plus, FT-IR Spectroscopy (Agilent Cary 630, Germany spectroscopy), X-ray diffraction (XRD)(SHIMDZU,7000, Japan), Scanning electron microscopy (SEM)(Bench Top SEM, JEOL Model: JCM-6000 PLUS, Japan).

3.3. Sample collection and preparation

3.3.1. Sample Collection and Preparation

Fresh Ginger was collected by purchasing from Jimma market, locally known as "Bishishe market". The Ginger was washed well and soaked in water to remove contaminants present in the skin. The cleaned Ginger was dried at room temperature to remove moisture content and the outer skin of *zingiber officinale* was peeled and the peeled ginger was cut into pieces and dried at room temperature. Then, the dried roots were crushed using mortar and pestle. To get crude root extract; the 5 g of powder was dissolved in 100 mL of distilled water under continuous magnetic stirring at 60 ^oC for 30 min. After time was completed the mixture was kept for a few minutes to cool down. Meanwhile, it was filtered by using Whatman no1 filter paper and stored at 4 ^oC in the refrigerator for further use [57].

3.4. Preliminary Phytochemical Screening of the Plant Extract

Test for flavonoids

i) 0.5 g of *zingiber officinale* root extract was mixed with 5 mL of distilled water and 1 mL of NaOH was added to the solution. The color change was observed, after that few drop of dilute HCl was added.

ii) 0.2 g of *z. officinale* root extract and 5 mL distilled water were mixed and 1 mL of 1% $AlCl_3$ was added and color change was observed.

Test for phenols

i) 50 mg of root extract and 5 mL of distilled water were mixed and a few drops of neutral 5% $FeCl_3$ solution was added and the color change was observed.

Test for Alkaloids

i) 2 mL of H_2SO_4 and a few drops of 40% formaldehyde mixture were added to 1 mL of plant root extract and were shaken. The color formed was observed [70].

Optimization of Some Parameters

Optimization of pH value

Table 3: Optimization of pH value at the same concentration of Zn $(NO_3)_2.6H_2O$ and Volume of root extract

The concentration of Zinc nitrate hexahydrate (in M)	The volume of Root Extract of *z.officinale* (mL)	pH value	Uv-reading	
			λ_{max} (nm)	Absorbance
0.1	20	6		
0.1	20	8		
0.1	20	9		
0.1	20	11		

Various parameters for nanoparticle synthesis were optimized by varying one parameter

and keep the other constant at a time to obtain the optimum values. Accordingly, the parameters such as concentration of precursor (Zn $(NO_3)_2.6H_2O$), the volume of plant extract, and pH were optimized in that by using the same concentration of precursor 0.1 M,0.1 M, and 0.1 M and the same volume of plant extract were mixed at different pH value (6,8,9 and 11) of the solution.

The absorbance of each different pH value was recorded at a wavelength range of 250 nm – 600 nm from UV-Vis spectroscopy.

Optimization of Precursor: Zinc nitrate hexahydrate

Constant volumes of plant extract (20 mL) were added to different amounts of concentration of precursor (0.5 M, 0.1 M, and 0.15 M) at optimized pH values. After this, the Wavelength and absorbance of each concentration were recorded.

Table 4: Optimization of Zinc nitrate hexahydrate concentration at constant volume of root extract as well as the same PH value

Concentration of $Zn(N0_3)_2.6H_2O$ in M	The volume of plant extract(in mL)	pH Value	Uv-Reading	
			λ_{max} (nm)	Absorbance
0.05	20	11		
0.1	20	11		
0.15	20	11		

The last optimization was an optimization of the volume of plant extract. In doing so, different volumes (10 mL, 20 mL, and 30 mL) of plant extract were mixed with a 0.1 M constant concentration of precursor at the same pH value and the UV-Vis result was recorded. During the experiment, the sharpest peak with the highest absorbance was preferred.

3.5. Synthesis of ZnO nanoparticles

50 mL of 0.1 M Zn $(NO_3)_2.6H_2O$ was prepared in a 250 mL volumetric flask and it was shaken until dissolved well and transferred to a beaker. After that, 20 mL of *zingiber officinale* root extract was added into the solution drop by drop under stirring. The pH of the solution was adjusted to pH 11 by adding 1 M NaOH until a white precipitate was formed. It was heated for 2 hrs at 70 ^{o}C and washed three times every 10 minutes using water and ethanol to remove impurities while using a centrifuge at 100 rpm. The product was collected and dried in Oven at 70 ^{o}C for 2 h. It was powdered by mortar and pestle and then stored in desiccators for further characterization.

3.6. Synthesis of Fe doped ZnO nanoparticles using *zingibber officinale* root extract

Fe doped ZnO nanoparticles were synthesized by weighing 7.4375 g of $Zn(NO_3)_2.6H_2O$ and dissolved in 250 mL distilled water in a 250 mL volumetric flask. 50 mL of $Zn(NO_3)_2.6H_2O$ solution was added to each of four beakers (I, II, III) from this volumetric flask. Then, 20 mL of root extract was added dropwise with continuous stirring into each of the beakers. Different percent of ferric chloride (1%, 3%, and 5%) were prepared and added to three of the beakers. The pH of the solutions was adjusted to pH =11 by Using 1 M NaOH and 0.1 M HCl. The solutions were stirred by a magnetic stirrer at a temperature of 70 ^oC for 2 h. The solutions were cool down for a few minutes. After that, they were filtered and centrifuged at 100 rpm and washed with either distilled water or Ethanol three times. The samples were dried in Oven for 2 hrs at a temperature of 70 ^oC. The dried samples were powdered by using a Mortar and pestle. The powdered samples were stored in a desiccator for further characterization and antimicrobial activity [57]. For the synthesis of Fe doped nanoparticles, three samples were prepared using the stoichiometric amounts of zinc nitrate hexahydrate and Ferric chloride.

Synthesis of 1% Fe-ZnO NCs

In this case, 1.4875 g of Zn $(NO_3)_2.6H_2O$ was dissolved in 50 mL of distilled water in a 100 mL volumetric flask and 1 g of $FeCl_3$ was dissolved in 100 mL of distilled water in a 25 mL volumetric flask. 50 mL Zn $(NO_3)_2.6H_2O$ (0.1 M), 10 mL $FeCl_3$ (0.01 M) and 20 mL of Ginger root extract were mixed into 250 mL beaker. Then the mixture was stirred continuously using a magnetic stirrer and the solution was kept at pH 11.0 by dropwise addition of 1 M sodium hydroxide (NaOH) with constant vigorous stirring with a magnetic stirrer for 2 h at room temperature. Then the resultant precipitant was centrifuged and washed repeatedly with distilled water followed by ethanol at 100 rpm for 10 min to eliminate the residual impurities. The precipitate was collected and kept at 60 ^oC in a hot air oven for 12 h. Then, the product of Fe doped ZnO NCs was powdered by pestle and mortar and stored at a desiccator for further characterization and antibacterial activity. The same procedure was undergone for each 3 and 5% Fe doping synthesis [98-99].

3.7. Characterizations of the Synthesized ZnO NPs and Fe- ZnO NCs

ZnO NPs and Fe-ZnO NCs were characterized by using Uv-vis spectrophotometry, FTIR spectrometry, X-ray Diffraction, and Scanning electron Microscopy.

3.7.1. UV-vis Spectra analysis

The absorption spectra of ZnO NPs and Fe-ZnO were obtained by using a Double beam UV-vis spectrophotometer (Model SPECORD 200/plus. ANALYTIK, JENA in 250-600nm range and distilled water was used as blank. The recorder data were plotted using Origin 8.0 and Origin 6.0 software.

3.7.2. Powder X-ray diffraction Studies

The XRD analysis was done at Jimma University, Technology Institute College of Engineering, at the Chemical Engineering department Laboratory. To identify the crystal phase and crystallite sizes of the synthesized nanocrystals. X-ray diffraction (XRD) studies were carried out using Shimadzu**,** XRD-6000 diffractometer at room temperature. The crystallinity and size of the NPs were acquired by using a powder x-ray diffractometer with Cukα radiation of a wavelength of λ = 1.5406 A^o in the 2θ range of 20^o – 70^o. Debye Scherrer's equation indicated in equation 1, was used to estimate the crystallite size.

$$D = \frac{k \times \lambda}{\beta \cos\theta} \quad ---------- Eq(1)[100]$$

Where D is the Crystallite size, is the X-ray source wavelength, β is the Full Width at Half Maximum (FWHM) of a peak, and θ is the Bragg diffraction angle.

The diffractions were compared with Joint Committee for Powder Diffraction Standards (JCPDS) library to account for crystalline structure.

3.7.3. FT-IR Spectral Analysis

Fourier Transmission Infrared Spectroscopy was conducted with the help of Agilent Cary 630 FTIR instrument which exists in the University of Jimma Chemistry department: at the Inorganic and Organic Research Laboratory. FT-IR spectroscopy was carried out to determine or identify the functional groups that might be involved in NPs formations in the range of 4000 – 400 cm^{-1} using KBr pellets. The synthesized Nps and Fe doped ZnO NCs were mixed with KBr powder

and pressed into a pellet for measurement. The background was corrected based on the spectrum from the reference pure KBr powder which was pressed into a pellet.

3.7.4. Evaluation of Antibacterial Activities of ZnO NPs and Fe doped ZnO NCs

Antibacterial assay of ZnO NPs and Fe doped ZnO NCs and Ginger root extract was performed by standard disc diffusion method. The Overnight Bacterial suspensions of Escherichia coli and Salmonella typhi (gram negative) and Staphylococcus aurus and Bacillus cerius (gram-positive) were used for the determination of antibacterial activities obtained from the Jimma University Biology department. To culture the bacteria Sterile Nutrient Agar was prepared as standard inoculum and added at 45 ^{o}C after solidification, 50 mg/mL of NP and root extract discs were kept on each plate and Gentamycin (50 mg/mL) was used as a reference drug. The two gram-negative strains namely, Salmonella typhi and Escherichia coli, and two gram-positive strains namely Staphylococcus aureus and Bacillus cereus) were performed using Muller-Hinton agar (MHA) medium by disk diffusion test (Kirby–Bauer test). 50 mg/mL of DMSO (30%), plant extract (100 µl) and ZnO NPs (50 mg/mL) was employed for the determination of antimicrobial activity. The inhibitory influence of the concentration of ZnO NPs is examined using a disc diffusion system by way of observing zone inhibition diameters (mm).

4. RESULT AND DISCUSSION

4.1. Synthesis of ZnO NPs and Fe-ZnO NCs

4.1.1. Mechanism for reduction and stabilization of NPs and Fe-ZnO NCs

The reduction of metallic ions by *zingiber officinale* is believed to be due to the presence of natural biomolecules such as flavonoids, alkaloids, and phenolic compounds [65]. Phytochemical analysis of *zingiber officinale* root extracts showed the presence of phenolic compounds reported by [67]. It is believed that the phenolic hydroxyl group acts as a reducing agent and forms an intermediate complex with the Zn^{2+} ion and finally reduce it to Zn^{o}, thereby themselves getting oxidized to corresponding carbonyl groups. Consequently, it becomes logical to reason that ZnO NPs prepared in the study should be stabilized by phenolic molecules through carbonyl groups [71]. ZnO NPs formed surrounded (capped) by a thin layer of other materials which is believed to be capping organic material from the aqueous root extract. These capping organic materials prevent the aggregation of ZnO NPs and thus provide extra stability to the synthesized ZnO NPs. The reduction of metallic ions was visually observed by a color change from light brown root extract to the white color of ZnO nanoparticles,(see appendix 6) which similar color change to the previous study[79] and from a white precipitate solution of ZnO NPs to red color precipitate (Fe doped ZnO solution) upon addition ferric chloride which confirmed the formation of the nanocomposite. During the synthesis of NPs, no other chemical reagent was introduced to the system because the active components in the extracts act as both reducing and capping agents [86].

4.2. Preliminary Phytochemical screening of the *zingiber officinale* root extract

The light brown aqueous extract was obtained from *zingiber officinale* root extract. Subsequently, the phytochemical constituents of the extracts were analyzed and the results were indicated in Table 5 below

Table 5: Phytochemical screening of *zingiber officinale* root extract.

S/no	Secondary metabolites	Tests	Observations	Remark
1	Phenols	Ferric chloride Test	A deep bluish green solution	+

2	Flavonoids	Alkaline reagent Test	Yellow coloration disappears on the addition of dilute HCl	++
3	Alkaloids	Marquis Reagent	Bluish Green color	+

+ =indicates the presence of phytoconstituents in extract ++= the presence of the highest phytochemical

During the phytochemical screening of *zingiber officinale* root extract, it was confirmed that the presence of the highest flavonoid content is observed by changing the color of root extract to yellow in alkaline reagent (NaOH) and after the addition of dilute HCl yellow color was disappeared. From it was generalized that the highest amount of flavonoids accumulated in ginger that responsible for antibacterial activity. In Testing phenolic contents ferric chloride is used as a testing agent. In this case, the deep bluish-green color was observed with some amount of phenolic group which is very important for bio reduction during synthesis of ZnO NPs and Fe doped ZnO NCs. The alkaloids group was tested by Marquis Reagent which was observed orange in color. This confirmed the presence of alkaloids in ginger.

4.2.1. Optimization of pH

Table 6: Optimization of PH value at the same concentration of Zn $(NO_3)_2.6H_2O$ and Volume of root extract

The concentration of Zinc nitrate hexahydrate (in M)	The volume of Root Extract of *z.Officinale* (mL)	pH value	Uv-reading	
			λ_{max} (nm)	Absorbance
0.1	20	6	375	1.498
0.1	20	8	380	1.322
0.1	20	9	370	1.259
0.1	20	11	365	1.755

From above Table 3, it was denoted that pH optimization was satisfied at pH =11. At this point, the sharpest peak with the highest absorbance was recorded at a wavelength of 365 nm with 1.755 absorbance which is below two.

4.2.1.2. Optimization of Precursor: Zinc nitrate hexahydrate

Table 7: Optimization of Zinc nitrate hexahydrate concentration at constant volume of root extract as well as the same pH value

Concentration of $Zn(N0_3)_2.6H_2O$ in M	The volume of plant extract(in ml)	pH Value	Uv-Reading	
			λ_{max} (nm)	Absorbance
0.05	20	11	377	0.040
0.1	20	11	368	0.391
0.15	20	11	378	0.079

Different concentrations of Zn $(NO_3)_2.6H_2O$ were seen at different wavelength ranges. 0.05 M concentration of $Zn(NO_3)_2.6H_2O$ was seen at 377 nm wavelength with 0.040 absorbance which is very low in concentration. This Confirmed that only a lesser amount of nanoparticles are synthesized at the position. For 0.1 M concentration of Zinc nitrate salt, nanoparticle synthesized can be seen at 368 nm with 0.391 absorbances. This is the preferred sharpest peak with the relatively highest absorbance of ZnO nanoparticles recorded and hence, it is selected for the next optimization. This absorption peak is very closer to the previous study in which the optical absorbance spectrum of ZnO NPs displayed an absorption peak at a wavelength of 370 nm [101,102]. Additionally, the synthesis of ZnO NPs is confirmed visually by the change in color of the solution into white precipitate.0.15 M concentration of precursor used to synthesis nanoparticle but due to it hasn't sharpness peak and low absorbance it cannot be selected for further reaction.

4.2.2. Optimization of Volume of Root extract of Ginger

Table 8: Optimization of Plant extract or *Zingiber officinale* root extract

The concentration of Zinc nitrate hexahydrate(in M)	The volume of Root Extract of Z.Officinale(mL)	pH value	Uv-reading	
			λ_{max} (nm)	Absorbance
0.1	10	11	369	1.553
0.1	20	11	377	1.456
0.1	30	11	376	0.9061

Table 9: Uv-Vis result of Fe-ZnO NCs

Uv-reading	**ZnO NPs**	1% Fe-ZnO	3% Fe-ZnO	5% Fe-ZnO
Wavelength	368 nm	370 nm	372 nm	374 nm
Absorbance	1.65	1.72	1.698	1.746

ZnO NPs and Fe-doped ZnO NPs were successfully synthesized using *Zingiber officinale* root extract as a reducing agent. The UV-Vis spectroscopy was observed in the wavelength range of 250 to 600 nm. Figures 2 & 3 below show the UV-Vis spectra of ZnO NPs as well as 1, 3, and 5 wt % Fe-doped ZnO. The result shows a broad peak at 368 nm for ZnO NPs, and then peaks were shifted towards higher wavelengths (redshift) due to Fe doping. This is indicated by the change in catalyst color from white to red. The highest absorption peak of 1% Fe-ZnO NPs is 370 nm with 1.72 absorbances; for 3% Fe-ZnO 372 nm absorption peak with 1.698 concentration and 374 nm absorption peak with 1.746 absorbances with the sharpest peak were recorded. From figure 2 and 3, it is clear that ZnO and Fe–ZnO shows absorption at 368 nm and 370 nm respectively as indicated in the previous literature at 350 nm and 360 nm [98]. The optical band gaps of the samples were determined. With the increase of Fe doping, the optical band gap of ZnO decreases as in the 3.120 eV, 3.00 eV, 2.97 eV, and 2.93 eV of 0,1, 3, and 5 wt% Fe-doped ZnO NCs respectively as shown in Appendix 6.

4.3. Structural analysis of synthesized nanoparticles

ZnO and Fe- ZnO nanocomposite were synthesized using *zingiber officinale* root extract as a reducing and capping agent.

4.3.1. UV-Vis Analysis

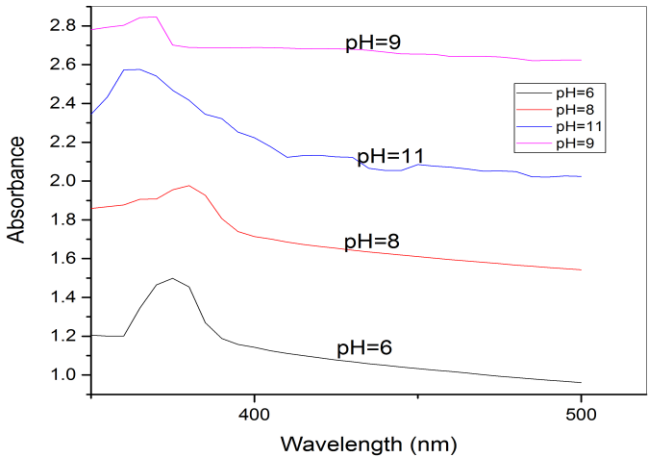

Figure 2: UV-Vis Graphical representation of ZnO NPs by using *Zingiber officinale* root extract

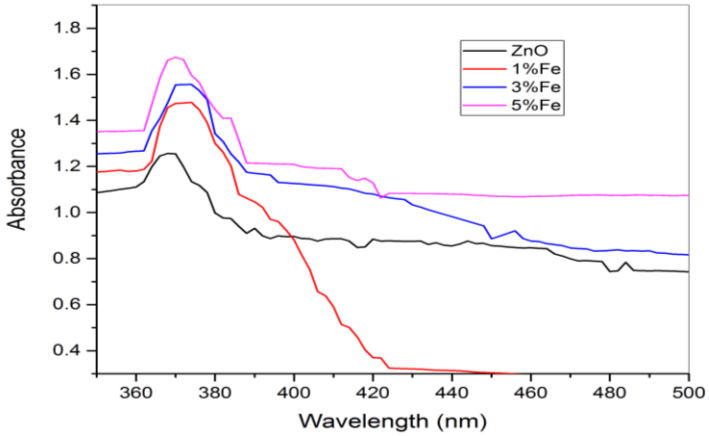

Figure 3*:* UV-Vis spectroscopy Fe doped ZnO nanoparticles using *Zingiber officinale* root extract

4.3.2. Characterization by FTIR spectroscopy

To detect the functional groups involved in the synthesis of NPs and nanocomposites, Fourier transforms infrared (FTIR) spectra of the native ginger extract, ZnO NPs, and Fe –doped ZnO NCs were performed using an FTIR which was examined in the range of 400–4000 cm−1.

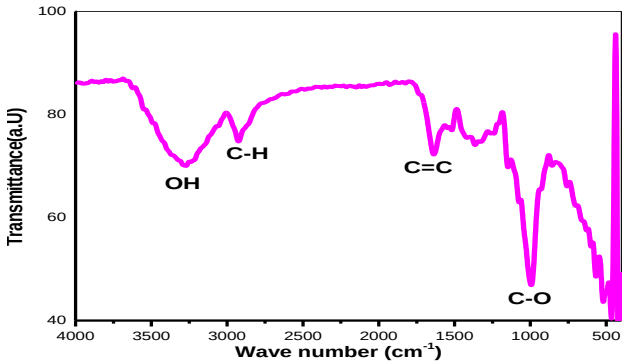

Figure 4a: FTIR spectra of *Zingiber officinale* root Extract

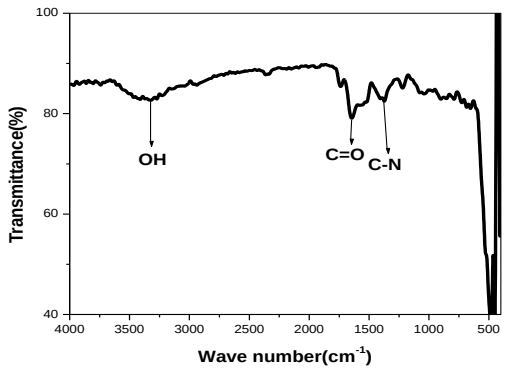

Figure 4b: FTIR spectra of undoped ZnO NCs

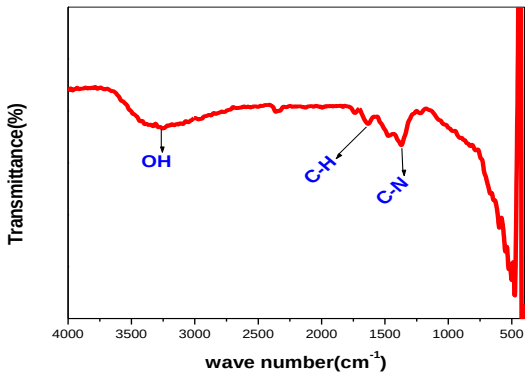

Figure 4c: FTIR spectra of 1%Fe doped ZnO NCs

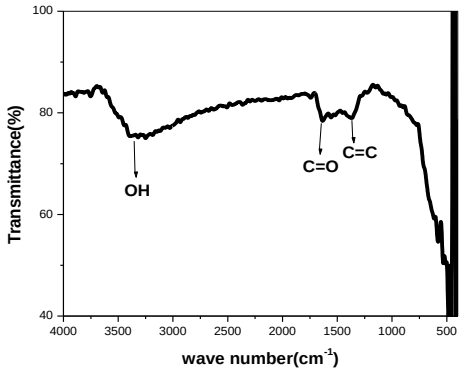

Figure 4d: FTIR spectra 3% Fe doped ZnO NCs

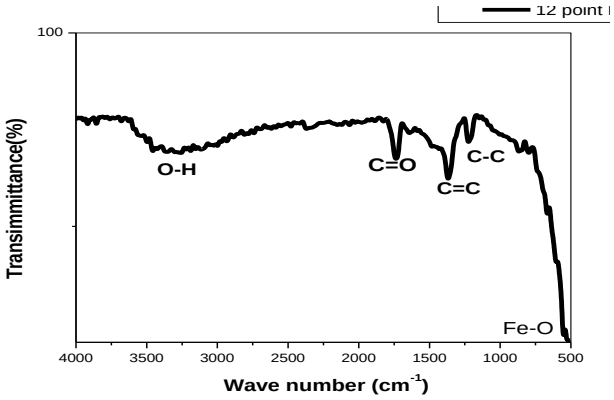

Figure 4e: FTIR spectra of 5% Fe doped ZnO NCs

Fig.4a-4e shows FTIR spectra of ZnO NPs and Fe doped ZnO NCs respectively. Information regarding functional groups, molecular geometry, and inter or intra-molecular interactions can be deduced from the FTIR spectrum of a compound. So, FTIR spectroscopy was employed to study the vibrational bands of the ZnO NPs and Fe- ZnO NCs at room temperature. The band frequencies occurring within the 1000 cm^{-1} range should be attributed to the bonds between inorganic elements [106]. The intense peaks shown in Figure 6b at 3347.15 cm^{-1} are due to O–H bond stretching of the solvent which is very close to other literature, that had been recorded at 3351.49 cm^{-1} and 3421.37 cm^{-1} [107].

The peaks below 1000 cm^{-1} showed the formation of nanoparticles[108]. The absorption peak in Figure 4b.at 678.35 cm^{-1} (ZnO NPs) which relative to the previous literature[109]. For 1% Fe doped ZnO NCs absorption peak seen at 609.12 cm^{-1}at and 575.87 cm^{-1}(3% Fe doped), as well as

519.9 cm^{-1}(5% Fe doped), shows the stretching frequency of Zn–O bond in zinc oxide. While absorption peak in Figure 4b at 471.6 cm^{-1} is characteristic stretching of Fe–O [110]. As Fe-atoms are slightly lighter than Zn atoms that's why their vibration requires low frequency and this clearly showed that Fe was successfully incorporated in ZnO crystal [111]. As Literature stated due to internal ionic vibrations Metal Oxide gives bands below 1000 cm^{-1}[112]. Then, in this work bands exist between 400 cm^{-1} and 600 cm^{-1} stretching ZnO NPs with doped was shown. Therefore, doping Fe ions in their absorption peaks were recorded between 471.6 and 547.918 cm^{-1}. The absorption peak in figure 4a of plant extract; at 2931.56 cm^{-1} -C=C- stretching of alkene and –C-H stretching of alkane, as well as phenolic group, have been shown at 1625.12 cm^{1}. Then, the absorption peak of plant extract, ZnO, and 1% Fe doped ZnO NCs confirmed the presence of –C=C- stretching conjugative alkene at 2931.56 cm^{-1}, 2357.15 and 2346.36 cm^{-1} respectively, and deviation of absorption bands for ZnO NPs. 678.9 cm^{-1} to 609.12 $cm^{-1}$of 1% Fe, 575.918 cm^{-1} 3% Fe and 547.918 cm^{-1} 5% Fe doped ZnO nanoparticles formed is due to transformation in bond lengths as a consequence of Fe doping onto ZnO. This can be supported by an earlier study [80].

4.2.3. X-ray diffraction Analysis of ZnO NPs and Fe doped ZnO NCs

X-ray diffraction analysis indicated that ZnO NPs and Iron doped ZnO NCs synthesized were with wurtzite phase and the entire diffraction peaks are supported by Joint Committee powder diffractions standard (JCPDS) data (card no.36-1451). The average crystallite size was calculated from the Debye- Scherrer formula [115].

$$\textbf{Scherer equation} = D = \frac{k\lambda}{\beta \cos\theta},$$

Where, k is cubic symmetry Scherer constant (the shape factor of the average crystallite and it can be considered k=0.90[91], λ = 0.15406 nm is the wavelength of the incident Cukα radiation; β =the line broadening at FWHM in radians, θ–Bragg's angle in degree half of 2θ and D is crystallite size.

The XRD pattern of synthesized ZnO NPs and Fe doped ZnO NCs was a range of 2θ = 20^{o} - 70^{o}their grain size were shown in (fig.8b-8e) below. All evident peaks could be indexed as the ZnO wurtzite structure (JCPDS data card:36-1401). wurtzite lattice parameters such as the values of d which is the distance between adjacent planes in the Miller indices (hkl).

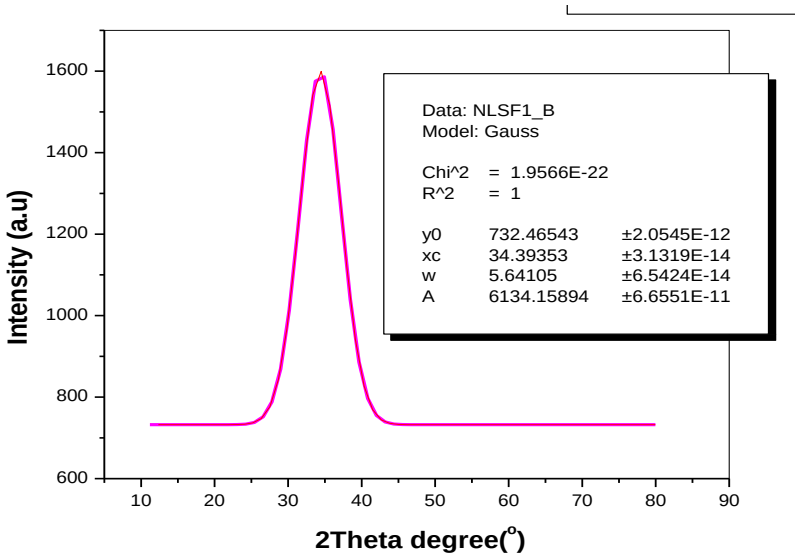

Figure 5: The XRD analysis shift of ZnO NPs to calculate crystallite size

Then: D = $/\beta 1/2cos\theta$, β= FWHM $\times 3.14 \frac{\text{radian}}{180} = 0.352 \times 3.14$ rad/ 180

$$\beta = 0.00614 \text{ degree}$$

$$D = \frac{0.94 \times 0.1506}{0.00614\text{degree} \times \cos\frac{34.394}{2}} = 23.2$$ (This is crystal size of ZnO NP)

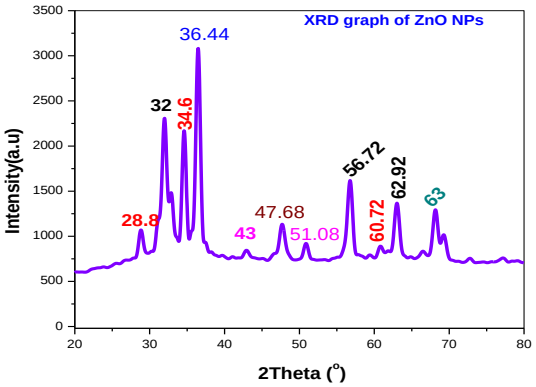

Figure 5b: XRD spectral analysis of ZnO NPs

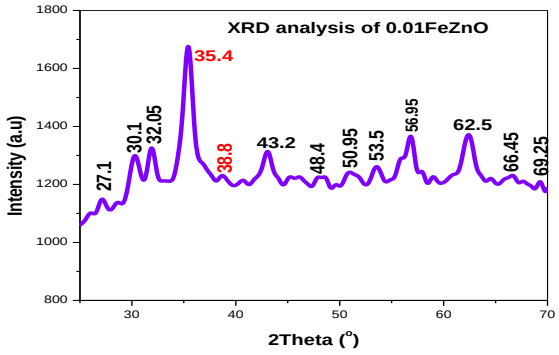

Figure 5c: XRD spectral analysis of 1% Fe- ZnO NCs

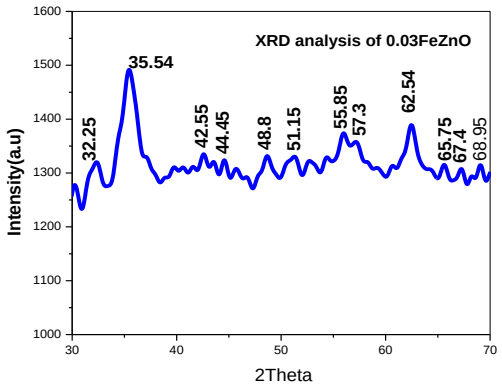

Figure 5d: XRD spectral analysis of 3%Fe ZnO NPs

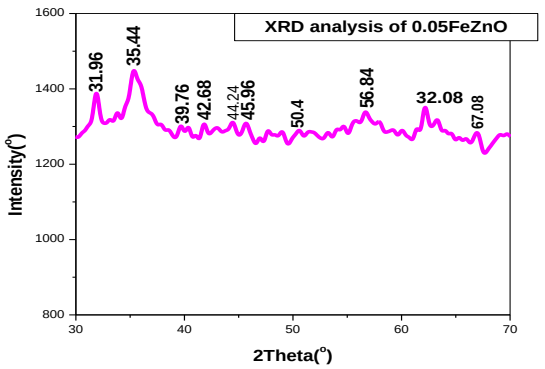

Figure 5e: XRD *spectral analysis of 5%Fe ZnO NC*

The 2θ calculated from the highest intense peak graph is 36. 4 supported by recent literature is 34.4306 [116] and β is 5.64 in radians as shown in fig.5a above. In this study, the XRD pattern displayed the existence of ZnO NP peaks found at 28.8°, 32°, 34.6°, and 36. 43°,44°,47.68°,51.08°,56.72°,60.72°, 62.29°and 63°, that is very close together which corresponds to the lattice plane (100), (002), (101), (102), (003), (110), (03) and (112), respectively. The crystallite size of ZnO NPs calculated by combining the data information. The intense and sharp peaks in the X-ray diffractogram showed that the synthesized ZnO NPs maintained their hexagonal wurtzite structure upon doping with iron. The small broadness in the major peak increases with the addition of dopant [110]. The obtained results also confirm the wurtzite structure of prepared ZnO NPs (figure 5b). The XRD pattern displayed the existence of 1%, 3%, and 5% Fe-ZnO NCs. These results of doping confirmed that as doping increases the intense peak decreases as shown in fig.5c – 5e above.

Table 10: Crystal size calculated for ZnO NPs and1% Fe doped ZnO NCs

2θ degree of ZnO NPs	Cos θ	FWHM	β	crystalline Size for intense peak (nm)	Miller indices,hkl	2θ Degree of 1% Fe-ZnO NCs	Cosθ	FWHM	β	crystalline size For intense peak (nm)
28	0.970				113	32.05	0.96			

							1			
32	0.961				100	35.44	0.952	0.415	0.00744	19.6
34.6	0.954				002	39.76	0.940			
36.4	0.949	0.352	0.0061	23.2	101	42.68	0.931			
47.66	0.9147				102	44.24	0.926			
51.08	0.90228				110	45.96	0.920			
56.72	0.879				003	50.4	0.904			

Table 11 : Crystal size calculated for Fe Doped ZnO

2θ degree 3% Fe-ZnO NCs	Cos θ	FWHM	β	crystallite size for intense peak (nm)	Miller indices,hkl	2θ degree 5% Fe-ZnO NCs	Cosθ	FWHM	β	Crystallite size for intense peak (nm)
30.1	0.965				100	32.25	0.960			
32.06	0.961				002	35.54	0.955	0.501	0.00872	16.32
35.5	0.952	0.451	0.00748	18.10	101	44.45	0.925			
38.8	0.943				102	48.8	0.910			
43.2	0.929				003	51.15	0.901			
48.4	0.912				110	55.85	0.884			

The average particle size of ZnO and Fe-ZnO NCs was 23 nm and 19.6 nm respectively, similar to [98-99]

4.2.4. Scanning electron microscopy (SEM) Characterizations

The SEM images of the synthesized general formula Zn1-xFexO samples are shown in Figures 6a and 6b Spongy network-type morphology is seen in the SEM images of all the samples. The origin of this spongy network-type structure could be assigned to the evolution of the volatile gases during the combustion process. In the SEM images, it seems that the fine nanosized particles are aggregated to form the irregularly shaped agglomerated/foamy particles.

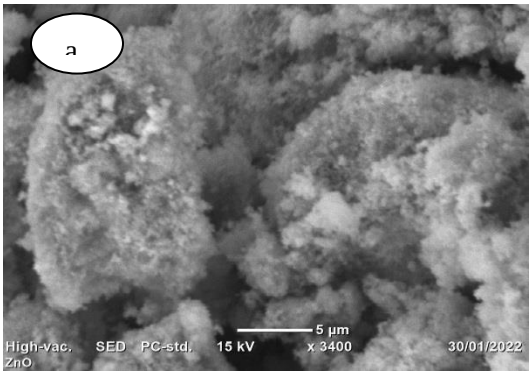

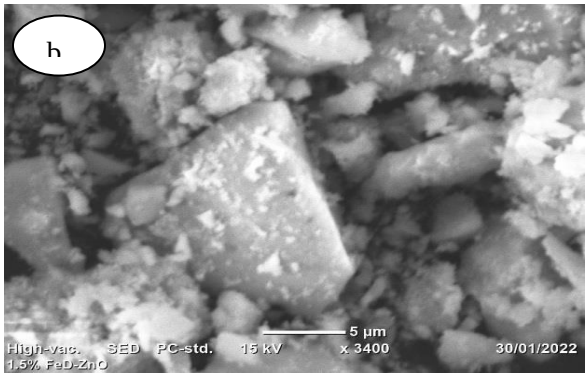

Figure 6a: SEM image of ZnO Np Figure 6b: SEM image of Fe-ZnO

The SEM images of ZnO NPs and Fe doped ZnO nanoparticles show that ZnO NPs nanoparticles are granular in size and have irregular spherical morphology. The morphology can also be affected by Fe doping in ZnO NPs. The results show that there is the dispersion of nanoparticles with less agglomeration as well as regular distribution of ZnO NPs due to Fe doping [112].

4.3. Antibacterial activity of ZnO NPs and Fe doped ZnO nanocomposite

The antibacterial activity of synthesized NPs and NCs was tested against four human pathogenic bacteria (two gram-negative strains namely, Salmonella typhi and Escherichia coli, and two gram-positive strains namely Staphylococcus aureus and Bacillus cereus). The results of the antibacterial assay are shown in Table 11 and Appendix 4

Table 12 : Antibacterial activity of green synthesized ZnO NPs against various pathogenic microorganisms.

Name of Organisms	Zone of inhibition(mm) ZnO NPs (50 mg/mL)	control		Root extract
		positive	Negative	
		Gentamycin	DMSO	
Staphylococcus aureus	14 mm	22 mm	NI	10 mm
E. coli	10 mm	23 mm	NI	7 mm
Bacillus cereus	15 mm	23 mm	NI	9 mm
Salmonella typhi	9 mm	20 mm	NI	8 mm

Within the process of comparative antibacterial test performed with green synthesized ZnO NPs and root extract at a concentration (50 mg/mL) and zone of inhibition (mm) as shown in Table 11. The comparative antibacterial test revealed green synthesized ZnO NPs have superior antibacterial activities than root extract of *zingiber officinale*; because of the capping agent (root extract) which binds the surface of nanoparticles (root extract + ZnO NPs), which increases the antibacterial activities. These outcomes have been similar to the previous report [112]. The Zone of inhibition varies depending on the microorganisms and combinations of Phyto compounds present on the surface of ZnO NPs. The green synthesized ZnO NPs were found to be more effective against Gram-positive bacteria than Gram-negative bacteria. The reason for the sensitivity difference between Gram-positive and Gram-negative bacteria could be Gram-positive bacteria have only an outer peptidoglycan layer which is not an effective permeability barrier. The lipopolysaccharides present in the outer membrane of Gram-negative bacteria provided resistance to antibacterial substances [112].

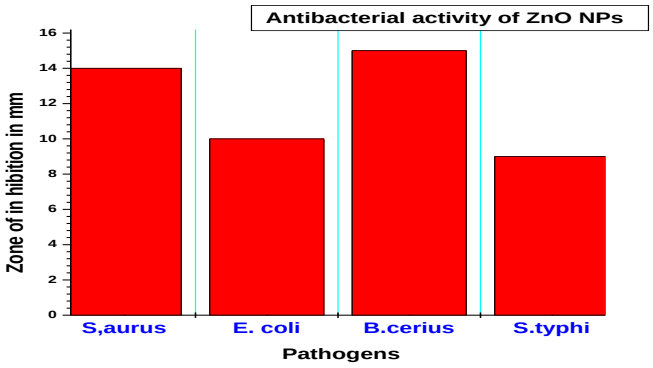

Table 13: Antibacterial activity of synthesis Fe doped ZnO NCs

Name of Organisms	Zone of inhibition(mm)				
	The concentration of Fe doped ZnO NCs			Positive	Negative
	1%Fe	3%Fe	5%Fe	Gentamicin	DMSO
	50 mg/mL	50 mg/mL	50 mg/mL		
Staphylococcus aureus	13 mm	14 mm	24 mm	22 mm	NI
E. coli	12 mm	13 mm	22 mm	23 mm	NI
Bacilus cereus	16 mm	18 mm	25 mm	23 mm	NI
Salmonella typhi	10 mm	11 mm	14 mm	20 mm	NI

Among these 4 pathogens, Gram-positive Bacilus cerius and gram-negative E.coli were sensitive in the zone of inhibition 25 mm and 24 mm respectively to ZnO (Doped with 5% Fe) when compared to the standard drug Gentamycin in Table 12. From these results, it is accomplished that the use of ZnO NPs and Fe doped ZnO nanoparticles has the potential for antibacterial activity against Gram-positive bacteria. Doped NPs showed high bactericidal activity because of the low energy band gap. With the decrease in the energy band gap, the surface to volume ratio increases, and this, in turn, increases bactericidal activity due to the generation of free radicals in the cell and enhanced binding forces penetration of metallic nanosized particles across the microsomal membrane can also be taken into account while explaining inhibition of oxidation-based biological process.

5. CONCLUSION AND RECOMMENDATIONS

5.1. Conclusion

A simple, biosynthetic, and low-cost approach for the synthesis of ZnO NPs and 1,3,5% Fe doped ZnO NCs utilizing the root extract of *zingiber officinale* plant is reported in this study. *Zingiber officinale* rhizome extract has secondary metabolite: alkaloid, phenolic, and flavonoid compounds. The qualitative phytochemical screening of *zingiber officinale* root extract was investigated and Zn metal binds to the polyphenolic group that undergoes bioreduction to produce ZnO nanoparticles as well as Fe-ZnO NCs. FTIR peaks confirmed the presence of chemical bonds that showed the involvement of ginger in the production of the nanoparticle. The XRD analysis of the intense and sharp peaks in the X-rays diffractogram showed that the synthesized ZnO NPs maintained their hexagonal wurtzite structure upon doping with iron. Then crystallite size of ZnO NPs and Fe-ZnO NCs was 23 nm and 19.6 nm which indicated that decreases in crystallite size were due to an increase in dopant concentration. ZnO, (1,3,5)%Fe doped ZnO shows absorption at 368 nm,370 nm,372 nm, and 376 nm respectively as indicated in the previous literature. Doping with Fe has shifted the absorption spectra of Fe–ZnO to a longer wavelength (red shift) as compared to the bulk of ZnO. From the SEM image, the morphology of ZnO NPs affected by Fe doping in ZnO NPs. The results show that there is the dispersion of nanoparticles with less agglomeration as well as regular distribution of ZnO NPs due to Fe doping. Antibacterial activity of ZnO NPs and Fe-ZnO NCs more successful over Gram-positive bacteria (S.aurus and B.cerius) than gram-negative bacteria (S.typhi and E.Coli). The produced ZnO NPs less effective on the four bacterial strains and as the dopant percent increases the activity of nanocomposite increases.

5.2. Recommendations

Gram-negative bacteria are most resistant to antibodies because of their impenetrable cell wall. To overcome bacterial infections and resist widespread of their existence; biosynthesis of Nanoparticles and their nanocomposite are carefully synthesized. Consequently, we can propose that ZnO and Fe-doped ZnO NPs at low dopant concentrations that can be prepared under the same conditions can be used as an ingredient for the dermatological applications in lotions, creams, ointments, or other biomedical applications. It is better if further investigation is conducted upon the plant extracts mediated synthesis of Fe-ZnO NCs.

REFERENCES

[1] Domany, El; A.E. Ahmed; T.M.Esssam; Farghali . A.A. Biosynthesis of Physico-Chemical Optimization of Gold Nanoparticles as Anti-Cancer and Synergetic Antimicrobial Activity Using *ostreatus* FungusPleurotus*, J.Appl.Pharm .science .**2018.*** 8(05), 119-128

[2] Bala, N , S. Saha, M. Chakraborty, M. Maiti, S. Das, R. Basu, P. Nandy, Green synthesis of zinc oxide nanoparticles using *Hibiscus subdariffa* leaf extract: effect of temperature on the synthesis, anti-bacterial activity, and anti-diabetic activity, *RSC Advances.***2015**. 5, 4993-5003.

[3] Goutam, S.P., G. Saxena, V. Singh, A.K. Yadav, R. N. Bharagava, KB Thapa, Green synthesis of TiO2 nanoparticles using leaf extract of Jatropha curcas L. for photocatalytic degradation of tannery wastewater, *Chem Eng. J*.**2018**.336, 386-96.

[4] Parthasarathy, G., M. Saroja, M. Venkatachalam, S. Shankar, V. Evangeline, Green synthesis of zinc oxide nanoparticles-review paper, *World J. Pharm. Pharm. Sci.***2016**. 5, 922-31.

[5] Prasad , Mittal AK, Chisti Y, Banerjee UC. Synthesis of metallic nanoparticles using plant extracts. *Biotechnol Adv*. **2013**. 31,346–356

[6] Garvasis , A. R., J., S.K. Oruvil, A. Joseph.Bio-inspired green synthesis of zinc oxide nanoparticles using Abelmoschus esculentus mucilage and selective degradation of cationic dye pollutants, *J.. Phy and Chem of Solids*. **2019**.127, 265-74.

[7] Vaseem , M., A. Umar, Y-B Hahn, ZnO nanoparticles: growth, properties, and applications In Metal oxide nanostructures, and their applications. *American Scientific Publishers* **2010**: pp: 1-36.

[8] Khan,M.M;M.H.Harunsani;A.L.Tan;Hojamberdier,M; Azamay.S;A.Norwayati. Antibacterial activities of zinc oxide and Mn-doped zinc oxide synthesized using *Melastoma malabathricum* (L.) leaf extract. *Bioprocess and Biosystem Eng.***2020**.https://doi org/10.1007/s00449-020-02343-3

[9] Raj , K.P; K. Sadaiyandi;-A. Kennedy; S. Sagadevan. Photocatalytic, and antibacterial studies of indium-doped ZnO nanoparticles synthesized by co-precipitation technique, *J. Mater.Sci: Mater in Elect.* **2017**. 28, 19025-37.

[10] Chitra K, Manikandan A, Arul Antony S. Effect of poloxamer on Zingiber officinale extracted green synthesis and antibacterial studies of silver nanoparticles. *J Nanosci Nanotechnol*. **2016**.16, 758–764.

[11] M. Ahmad, E. Ahmed, Y. Zhang, N. Khalid, J. Xu, M. Ullah, and Z.L. Hong, Preparation of highly efficient Al-doped ZnO photocatalyst by combustion synthesis, *Curr. Appl. Phys*. **2013**.13, 697-704.

[12] Kanemitsu , Y., K. Suzuki, Y. Nakayoshi, Y. Masumoto, Quantum size effects and enhancement of the oscillator strength of excitons in chains of silicon atoms, *Phys. Rev. B.* **1992**. 46, 3916.

[13] Salehnezhad , L., A. Heydari, M. Fattahi. Experimental Investigation and Rheological Behaviors of Water-Based Drilling Mud Contained Starch-ZnO Nanofluids through Response Surface Methodology, *J. Mol. Liq*. **2019.**276. 417-430.

[14] Fattahi , M., M. Kazemeini, F. Khorasheh, A.M. Rashidi. Morphological Investigations of Nanostructured V_2O_5 over Graphene Used for the ODHP Reaction: From Synthesis to Physiochemical Evaluations, *Catal. Sci. Tech*. **2015**.5(2), 910-924.

[15] Nie, L., L. Gao, P. Feng, J. Zhang, X. Fu, Y. Liu, X. Yan, T. Wang, Three-dimensional functionalized tetrapod-like ZnO nanostructures for plasmid DNA delivery, *Small*. **2006**. 2, 621-5.

[16] Hayati, F., A. A. Isari, M. Fattahi, B. Anvaripour and S. Jorfibc. Photocatalytic decontamination of phenol and petrochemical wastewater through ZnO/TiO2 decorated on reduced graphene oxide nanocomposite: Influential operating factors, mechanism, and electrical energy consumption, *RSCAdvances* .2018, 8(70), 40035-40053.

[17] Lam .S.; Ch. H.; Sin. J. Green synthesis of magnetic Fe-doped ZnO nanoparticles via *Hibiscus rosa-sinensis* leaf extracts for boosted photocatalytic, antibacterial, and antifungal activities. *Materials Letter*.**2019**.doi.https://doi.org/10.1016/j.matlet 2019.01.116

[18] Shojaie , A., M. Fattahi, S. Jorf, B. Ghasemi. Synthesis and evaluations of Fe3O4-TiO2-Ag nanocomposites for photocatalytic degradation of 4-chlorophenol (4-CP): Effect of Ag and Fe compositions, *Int. J. Ind. Chem*. **2018**.9 (2), 141-151.

[19] Patidar , D., A. Kaswan, N. S. Saxena and K. Sharma, Monodispersed ZnO nanoparticles and their use in heterojunction solar cell, Sci. World J., **2013**, DOI: 10.1155/2013/ 260521.

[20] Ansari SA, Khan MM, Ansari MO, Lee J, Cho MH, Biogenic synthesis, photocatalytic, and photoelectrochemical performance of Ag–ZnO nanocomposite, *The J. Phy. Chem. C*, **2013**. 117, 27023-30.

[21] Peng, J.M., J.C. Lin, Z.Y. Chen, M.C. Wei, Y.X. Fu, S.S. Lu, D.S. Yu, W. Zhao, Enhanced antimicrobial activities of silver- nanoparticle decorated reduced graphene nanocomposites against oral pathogens, *Mater Sci and Eng*: C. **2017**,71, 10-6.

[22] Takahashi , C., N. Matsubara, Y. Akachi, N. Ogawa, G. Kalita, T. Asaka, M. Tanemura, Y. Kawashima and H. Yamamoto, Visualization of silver- decorated poly (DL-lactide-co-glycolide) nanoparticles and their efficacy against Staphylococcus epidermidis, Mater. *Sci. and Engineering*: C. **2017.** 72, 143-9.

[23] Shojaie , A, , M. Fattahi, S. Jorfi, B. Ghasemi. Hydrothermal Synthesis of Fe-TiO_2-Ag Nano-Sphere for Photocatalytic Degradation of 4- Chlorophenol (4-CP): Investigating the effect of hydrothermal temperature and time as well as calcination temperature, *J. Environ. Chem. Eng*. **2017**.5 (5), 4564-4572.

[24] Dias , H.B., M.I.B. Bernardi, V.S. Marangoni, A.C. de Abreu Bernardi, A.N. de Souza Rastelli, A.C. Hernandes, Synthesis, characterization, and application of Ag-doped ZnO nanoparticles in a composite resin, *Mater. Sci. and Eng.: C*, **2019**.96, 391-401.

[25] Hassanpour, M, H;-Safardoust-Hojaghan, M;- Salavati-Niasari, A;- Yeganeh-Faal, Nano-sized CuO/ZnO hollow spheres: synthesis, characterization and photocatalytic performance, *J. Mater.Sci: Mater in Elect*. **2017**. 28, 14678-84.

[26] Velmurega.S.; K.E.; Kathiravan.V.; S.R.; Raj Adikala. G: Bio-approach: Plant mediated synthesis of ZnO nanoparticles and their catalytic reduction of methylene blue and antimicrobial activity, *Adv. Powder tech*.**2015**.26, 1639-1651

[27] Chen. D.; et al.Preparation and photocatalytic properties of ZnO nanoparticles by microwave-assisted ball milling.Ceramics Inte.**2016**.42,3692-3696.

[28] A.U. Khan, Q. Yuan, Z.U.H. Khan, A. Ahmad, F.U. Khan, K. Tahir, M. Shakeel, S. Ullah, An eco-benign synthesis of AgNPs using the aqueous extract of Longan fruit peel: Antiproliferative response against human breast cancer cell line MCF-7, antioxidant and photocatalytic deprivation of methylene blue, *J. Photochem. Photo B: Biology*, **2018**. 183, 367-73.

[28] Shakeel, M. M. Arif, G. Yasin, B. Li, A.U. Khan, F.U. Khan, M.K. Baloch, Hollow mesoporous architecture: A high-performance Bifunctional photoelectrocatalyst for overall water splitting, *Electrochimica Acta*,**2018**. 268, 163-72.

[29] Khatami, M., R.S. Varma, N. Zafarnia, H. Yaghoobi, M. Sarani, V.G. Kumar, Applications of green synthesized Ag, ZnO, and Ag/ZnO nanoparticles for making clinical antimicrobial wound-healing bandages, *Sustainable Chem and Pharma*,**2018**.10, 9-15.

[30] Zhang , Y., J. Mu, One-pot synthesis, photoluminescence, and photocatalysis of Ag/ZnO composites, *J. Colloid Interface Sci*. **2007**. 309, 478-84.

[31] Uda. M.N.A, et al. Preliminary Studies on Antimicrobial Activity of Extracts from aloe Vera Leaf, Citrus Hystrix Leaf, Zingiber Officinale, and Sabah Snake Grass Against Bacillus Subtilis, *Matec webof conf*. **2017**.150,06042

[32] Nageswara Rao L, Kamalakar D, Biomedical Applications of Plant mediated green synthesis of Metallic Nanoparticles - A Theoretical Study, *J.of Chem, Biolog andPhysi Scien.***2014**, 4(4), 3819-3824.

[33] Shah. R.K, et al, Synthesis and Characterization of ZnO Nanoparticles Using Leaf Extract of Camellia sinesis and Evaluation of their Antimicrobial Efficacy: *Int.J.curr.microbiol.App.scie*.**2015**.4(8),444-450

[34] Devi , B. S. R., R. Raveendran, and A. V. Vaidyan, Synthesis and characterization of Mn2+-doped ZnS nanoparticles, *Pramana* **2007**.68, 679–687.

[35] Ghule. K.; G. AV.; Chen. BJ.; Ling YC. Preparation and characterization of ZnO nanoparticles coated paper and its antibacterial activity study. *Green Chemistry*. **2006**.8(12), 1034-41.

[36] Gatti, A.; T. D.; G. A.; M. S.; Capitani, F. Investigation of the presence of inorganic micro- and nanosized contaminants in bread and biscuits by environmental scanning electron microscopy. *Crit Rev Food Sci Nutr* **2009**.49(3):275-82

[37] Rahiman, A.Ket.al. Invitro antioxidant and antidiabetic activities of zinc oxide nanoparticles synthesized using different plant extracts: *Bioprocess and Biosystem Engineering* .**2017.** 40, 943–957

[38] Chitra K, Reena K, Manikandan A, et al. Antibacterial studies and effect of poloxamer on gold nanoparticles by zingiber officinale extracted green synthesis. *J. Nanosci Nanotechnol*. **2015**. 15, 4984–4991

[39] Parveen. M, Ahmad F, Malla AM, et al. Microwave-assisted green synthesis of silver nanoparticles from Fraxinus excelsior leaf extract and its antioxidant assay. *Appl Nanosci*. **2016**.6, 267–276.

[40] Ghosh, A.K.; Banerjee, S.; Mullick, H.I.; Banerjee, J. *Zingiber officinale*: A Natural Gold, *Int. J of bioengi. Sci.*, **2011**.*2*, 283-294.

[41] Li. Q.; Mahendra S.; Lyon DY.; Brunet L.; Liga MV.; Li D.; Alvarez PJJ. Antimicrobial nanomaterials for water disinfection and microbial control: Potential applications and implications. *Water Res*. **2008.**4.2(18), 4591-602.

[42] Matheswaran, M.et.al. The strategy of metal iron doping and green-mediated ZnO nanoparticles: dissolubility, antibacterial and cytotoxic traits, *Toxicol res*.**2017**.6,854

[43] Hatamie , A., A. Khan, M. Golabi, A. P. Turner, V. Beni, W. C. Mak, and O. Nur, Zinc oxide nanostructure-modified textile and its application to biosensing, photocatalysis, and as antibacterial material, *Langmuir*, **2015**, 31, 10913–10921.

[44] Alagaris, A., Introduction to nanomaterials:http:// www.research gate.net/publication/accessed on December **2011**)

[45] Sirelkhatim , A., S. Mahmud, A. Seeni, N. H. M. Kaus, L. C. Ann, S. K. M. Bakhori and D. Mohamad, Review on zinc oxide nanoparticles: antibacterial activity and toxicity mechanism, *Nano-Micro Lett*., **2015**, 7,219–242.

[45] Rekha , K., M. Nirmala, M. G. Nair, and A. Anukaliani, Structural, optical, photocatalytic and antibacterial activity of zinc oxide and manganese doped zinc oxide nanoparticles, *Physica B*, **2010**, 405, 3180–3185.

[46] Radzimska. A and T. Jesionowski, Zinc oxide —from synthesis to application: a review, *Materials*, **2014**,7,2833–2881.

[47] Iravani , S., Green synthesis of metal nanoparticles using plants, *Green Chem*., **2011**, 13, 2638–2650.

[48] M. H. Koupaei, B. Shareghi, A. A. Saboury, F. Davar, A. Semnani, and M. Evini, Green synthesis of zinc oxide nanoparticles and their effect on the stability and activity of proteinase K, *RSC Adv*., **2016**, 6, 42313–42323.

[49]Yun, S., et al., Improvement of ZnO nanorod-based dye-sensitized solar cell efficiency by Al-doping. *J. of physics and chemistry of solids,***2010**.*71(2),1724-1731*

[50] Jayaseelan , C., A. A. Rahuman, A. V. Kirthi, S. Marimuthu, T. Santhoshkumar, A. Bagavan and K. B. Rao, Novel microbial route to synthesize ZnO nanoparticles using Aeromonas hydrophila and their activity against pathogenic bacteria and fungi, *Spectrochim. Acta, Part A*, **2012**, 90, 78–84.

[51]. Yayapao, O., et al., Ultrasonic-assisted synthesis of Nd-doped ZnO for photocatalysis. *Materials Letters*, **2013**. 90, p. 83-86.

[52]Yu, W., J. Zhang, and T. Peng, New insight into the enhanced photocatalytic activity of N-, C- and Si-doped ZnO photocatalysts. *Applied Catalysis B: Environmental*, **2016**. 181, p. 220-227.

[53] Jayanthi P, Gaithuilung R, Kazingmei P. Physicochemical analysis for reclamation of soils of Tingroi Hills in Lunghar, Ukhrul District, Manipur, India. *Universal J .Environ Res Technol*.**2015**.5, 101–111.

[54] Pattanayak S, Mollick MMR, Maity D, et al. Butea monosperma bark extract mediated green synthesis of silver nanoparticles: characterization and biomedical applications. *J. Saudi Chem Soc*.**2017**.21, 673–684.

[55]Nikokavoura, A. and C. Trapalis, Alternative photocatalysts to TiO2 for the photocatalytic reduction of CO_2. *Applied Surface Science*, **2017**. 391: p. 149-174.

[56]. Elumali,k;S.R;velmuragan.S;kathiravan.v. Bio-approach: Plant-mediated synthesis of ZnO nanoparticles and their catalytic reduction of methylene blue and antimicrobial activity. *Advanced Powder Technology*, **2015**.26, 1639–1651

[57]Ananrnd Rej.L.F.A;E.j.Biosynthesis and Characterization of Zinc oxide nanoparticles using Root Extract of *Zingiber officinale.Oriental J. of chemistry*,**2015**. *31,51-56*

[58]. Sawai J, Quantitative evaluation of antibacterial activities of metallic oxide powders (ZnO, MgO, and CaO) by conduct metric assay, *Journal of Microbiological Methods*, **2003**.54, 177–182

[59] Cynthia Mason, Singaravelu Vivekanandhan, Manjusri Misra, Amar Kumar Mohanty, Switchgrass *(Panicum virgatum)* Extract Mediated Green Synthesis of SilverNanoparticles, *World J. of Nano Sci. and Engi.,* **2012**, 2,47-52.

[60] Akl , M, Nidà M. Amany O, Biosynthesis of Silver Nanoparticles using *Olea europaea* Leaves Extract and its Antibacterial Activity, *Nanosci. and Nanotechn.,***2012**, 2(6), 164-170.

[61] Saurabh. N.S.et al. Antimicrobial activity of ginger and onion extract against enteric pathogens, *J.of pharma. And Photochem.* **2018**.7(8), 2653-2656.

[62]Li, J. and N. Wu, Semiconductor-based photocatalysts and photoelectrochemical cells for solar fuel generation: a review. *Catalysis Sci. & Techno.,***2015**. 5(3), p. 1360-1384.

[63] Arawande, J.O; A.A; Alademeyin, J.O.Extractive Value and Phytochemical Screening of Ginger(*zingiber officinale*) and Turmeric (*curcuma longa*) UsingDifferent Solvents. *Intern. J. of Traditional and Natural Med.,***2018**. *8(1), 13-222*

[64] Jones N, Ray B, Ranjit KT, Manna AC, Antibacterial activity of ZnO nanoparticle suspensions on a broad spectrum of microorganisms, *FEMS Microbiology Letters,* **2008**. 279, 71–76.

[65] Rosfarizan ,A.S; M.R. Abdul. et.al ZnO-Ag Core-Shell Nanocomposite Formed by Green method using Essential Oil of Wild Ginger and Their Bactericidal and Cytotoxic Effects: *Appl surfacesci*.**2016**.16, 31060-1

[66] Lampronti I, Khan MTH, Bianchi N, Borgatti M, Gambar R, Inhibitory effects of medicinal plant extracts on interactions between DNA and transcription factors involved in inflammation, *Minerva Biotecnologica*, **2004**, 16, 93–99.

[67] Bassey, F. I; Osabor, V. N. ; Umoh,U. U. Phytochemical Screening and Quantitative Evaluation of Nutritional Values of *Zingiber officinale* (Ginger). *American Chemical Sci. J,* **2015**,*8(4), 1-6*

[68]. Aleem.M.et al. Botany, phytochemistry and antimicrobial activity of ginger (*Zingiber officinale*): A review. *Intern. J. of Herbal medicine*,**2020**, 8(6), 36-49

[68]Wungu. T.D.K. et.al**.**Synthesis, Characterisation, and Density Functional TheoryStudy of Encapsulated Bioactive Components of Ginger.*Pertanika J. Sci. & Technol*..**2021**, 29 (4), 2645 – 2657.

[69] Alkandahri,Y.M; K. H.A; Fikayuniar,L. Antibacterial Activity of *Zingiber officinale* Rhizome. *Intern.J. of Psychological Rehabilitation,* **2020**. 24, 1475-7192

[70]Kamali.D.et.al. Investigation of phytochemical composition and antioxidant activity of *zingiber officinale.World J.of pharmaceutical Research,* **2021**,*8, 1389-1401*

[71]. Gunalan, S; Silvaraj, R.; Rajendran, V.; Green synthesized ZnO nanoparticles against bacterial and fungal pathogens progress in Natural science*: Materials International,***2012**,*22,693-70.*

[72].Nagajyothi,P.;An,T.M.;D.S.,Lee,J.-i.;Lee,D.J.;Lee,K.,Green route biosynthesis, characterization, and catalytic activity of ZnO nanoparticles.*Materials Letters*,**2013**,*108,160-163*.

[73].Gananasangeeetha, D.; Thambavani, D.S., Biogenic production of ZnO nanoparticles using Acalyypha indica, *J.of Chemic., Biolo. and physi sci.(JCBPS)*,**2013**,*4,238*

[74]. Gananasangeeetha, D.; Thambavani, S.D., Facile and eco-friendly method for the synthesis of ZnO nanoparticles using Azadirachta and Emblica.*Intern. J. of pharma. Sci. and research*,**2014**, *5, 2866.*

[75]. Ramesh, P.; Rajendran, A.; Meenakshisundiran, M., Green synthesis of ZnO nanoparticles using flower extract cassia auricualata.*J. of nanosci. and Nanotechn.*,**2014**,*2,41-45*.

[76]. Naeem, M.; Hasanian, S.; Mumtaz, A., Electrical transport and optical studies of ferromagnetic cobalt doped ZnO nanoparticles exhibiting ametal insulator transition.Journal of physics*:Condensed Matter*,***2007***,*20,2866.*

[77]. Ecambram, S.; Iikubo, Y.; Kudo, A., Combustion synthesis and photocatalytic properties of transition metal incorporated ZnO.*J. of alloys and compounds*,**2007**,*433,237-240.*

[78].Ahmed, N. Abd.; Abdul Jalill ,R.D.; Slman,Dh.K. Biosynthesis of zinc oxide nanoparticles by hot aqueous extract of allium sativum plants: *J. Pharm. Sci. & Res*. **2018**, 10(6), 1590-1596

[79]. Datta.; et.al. Green Synthesis of Zinc Oxide Nanoparticles Using Parthenium hysterophorus Leaf Extract and Evaluation of their Antibacterial Properties: *J. of Biotechn& Biomater*,**2017,** 7:3,

[80]. Vedhi.C.; Karpagavinayagam, P.; Kavitha, M.; Saravanadevi, K.; Saminathan, K. Biosynthesis of ZnO and Ag-doped ZnO nanoparticles from Vitis vinifera leaf for antibacterial, photocatalytic application: *Materials Today: Proceedings* xxx (xxxx) **2020**

*[81]*Shah, R.K.; Boruah, F.; Parween, N**.**Synthesis and Characterization of ZnO Nanoparticles using Leaf Extract of Camellia sinesis and Evaluation of its antimicrobial activities: *Int.J. Curr. Microbiol.App.Sci.* **2015**, 4(8): 444-450

[82].Velmurugan, S, et.al. Bio-approach: Plant mediated synthesis of ZnO nanoparticles and their catalytic reduction of methylene blue and antimicrobial activity: *Advanced Powder Technology*, **2015**, 26, 1639–1651

[83].Elangovan, N.; et.al. Antimicrobial Activity of Green Synthesized Zinc Oxide Nanoparticles from *Emblica Officinalis: Int. J. Pharm. Sci. Rev. Res*., **2015**, 33(2), 110-115

[84].Fun,Ch.S.et.al: Comparative Evaluation of AntibacterialEfficacy of Biological Synthesis of ZnONanoparticles Using Fresh Leaf Extract and fresh Stem-Bark of *Carica papaya: Nano Biomed Eng*,**2019**, 11(3),264-271

*[85]*Matheswaran, M.; Harshiny, M.; Devi, S.A.; Gopinath, P. Strategy of metal iron doping and green-mediated ZnO nanoparticles: dissolubility, antibacterial and cytotoxic traits:*Toxicol. Res*., **2017**, 6, 854

[86].Biosynthesis and Characterization of Zinc Oxide Nanoparticles using Root Extract of *Zingiber officinale:Oriental journal of chemistry*.**2015**, 31, No. (1): 51-56

*[87]*Lam, S-M.; Chai, HY.; Sin, Ch-ch. Green synthesis of magnetic Fe-doped ZnO nanoparticles via *Hibiscus rosa sinensis* leaf extracts for boosted photocatalytic, antibacterial, and antifungal activities: *Materials*

*Letters***, 2019**

[88]. Zhu, D., et al., High-performance self-powered/active humidity sensing of Fe-doped ZnO nanoarray nanogenerator.Sensors and Actuators *B: Chemical*,**2015**. 213, p. 382-389.

[89]. Jandaik, S.; Sharma, N.; Kumar, S.; Chitkara, M.; Sandhu, I.S. Synthesis, characterization and antimicrobial activity of manganese- and iron-doped zinc oxide nanoparticles*: J. of Exper. Nanosci.*, **2016**, 11, No. 1, 5471

[90][91]. Muşat,v.et.al.Fe-Doped ZnO Nanoparticles: Structural, Morphological, Antimicrobial and Photocatalytic Characterization: Advanced Materials Research, **2016**, 1143, 233-239

[92] Brayner R, Ferrari-Illiou R, Briviois N, Djediat S, Benedetti MF, Fievet F, Toxicological impact studies based on *Escherichia coli* bacteria in ultrafine ZnO nanoparticles colloidal medium, *Nano Letters*,**2006**.6, 866–870.

[93][94]. Khan,M.M.; Harunsani,M.H.; Tan,AL.; Hojamberdiev,M.; Azamay,S.; Ahmad,N.Antibacterial activities of zinc oxide and Mn-doped zinc oxide synthesized using *Melastoma malabathricum* (L.) leaf extract: *Bioprocess and Biosystems Engin.*,**2020**

[95][96]. Han, R.; Jiang, L.; Wang, P.Biosynthesis of Zinc oxide nanoparticles and their application for antimicrobial treatment of burn wound infections: *Mater. Res. Express*,2020. 7, 095010

[97].El-Sayed,A.et.al**.** Biosynthesis and Anti-Mycotoxigenic Activity of *Zingiberofficinale* Roscoe-Derived Metal Nanoparticles: *Molecules* **2021**,*26*, 2290.

[98[99]. Jan,F.A,et.al. Exploring the environmental and potential therapeutic applications of Myrtus communis L.

assisted synthesized zinc oxide (ZnO) and iron-doped zinc oxide (Fe-ZnO) nanoparticles: *J. of Saudi Chemi. Soci.*, **2021**, 25, 101278

[100][101][102]. Han, R.; Jiang, L.; Wang, P.Biosynthesis of Zinc oxide nanoparticles and their application for antimicrobial treatment of burn wound infections: *Mater. Res. Express*, 2020. 7, 095010

[103-105]. Muthukumar,H.et.al. Effect of iron-doped Zinc oxide nanoparticles coating in the anode on current generation in microbial electrochemical cells: *Intern. J. of hydrogen e n e r g y*,**2018**.xxx. I-10

[106-111].Kunj, S.Defects and dopant alliance towards bound magnetic polarons formation and mixed magnetic characteristics in Fe doped ZnO nanoparticles: *J. of Indust. and Enginee. Chemi.* 2019, xxx , xxx–xxx

[112].Laurenti, M.; Cauda, V.; Barui, S.; Carofiglio, **M,** Doped Zinc Oxide Nanoparticles: Synthesis, Characterization and Potential Use in Nanomedicine: *Appl. Sci.* **2020**, *10*, 5194,

Appendix 1

zingibber Officianale root was extracted in the following procedure:

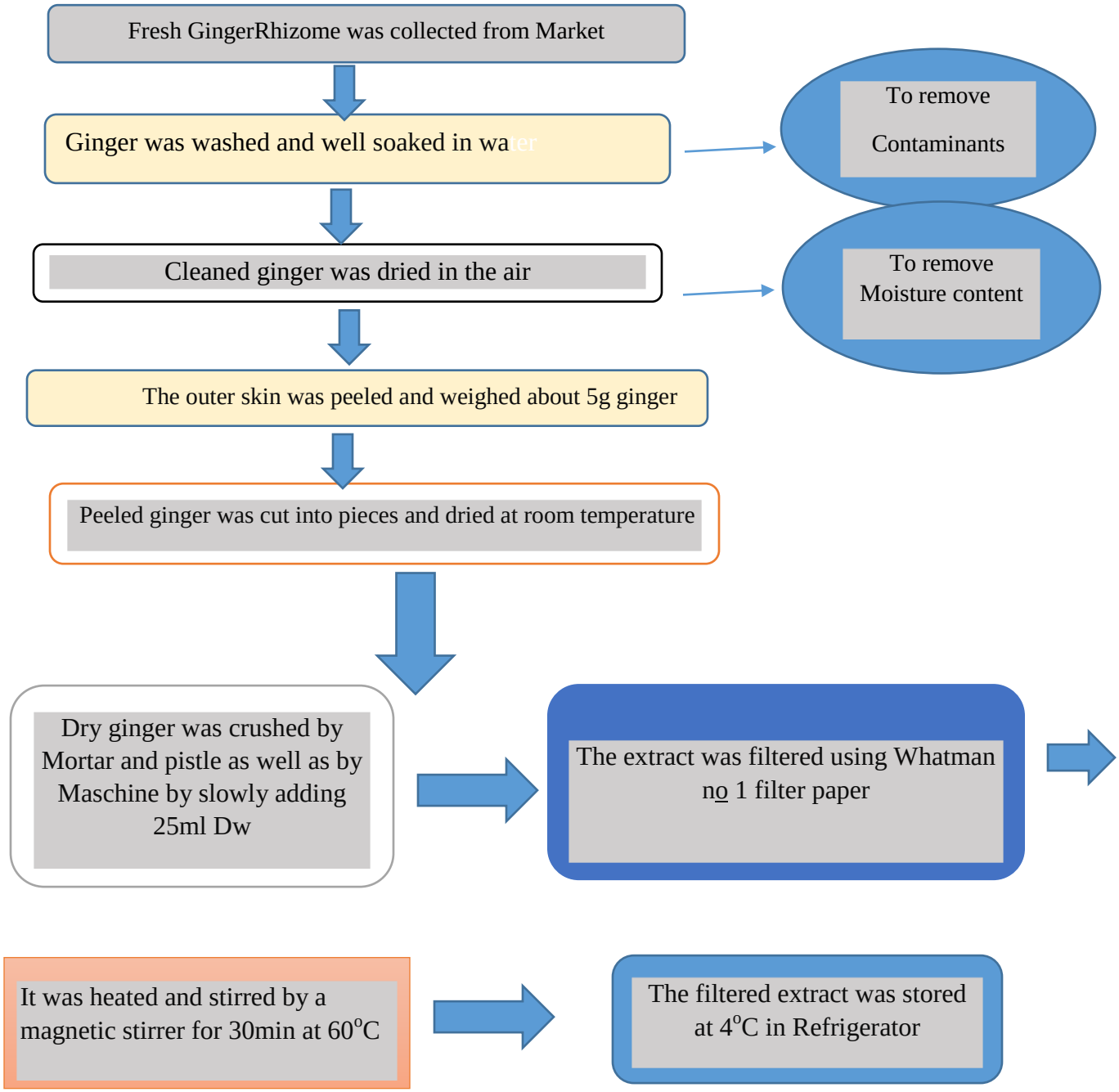

Appendix 2

The procedure of ZnO nanoparticle synthesis

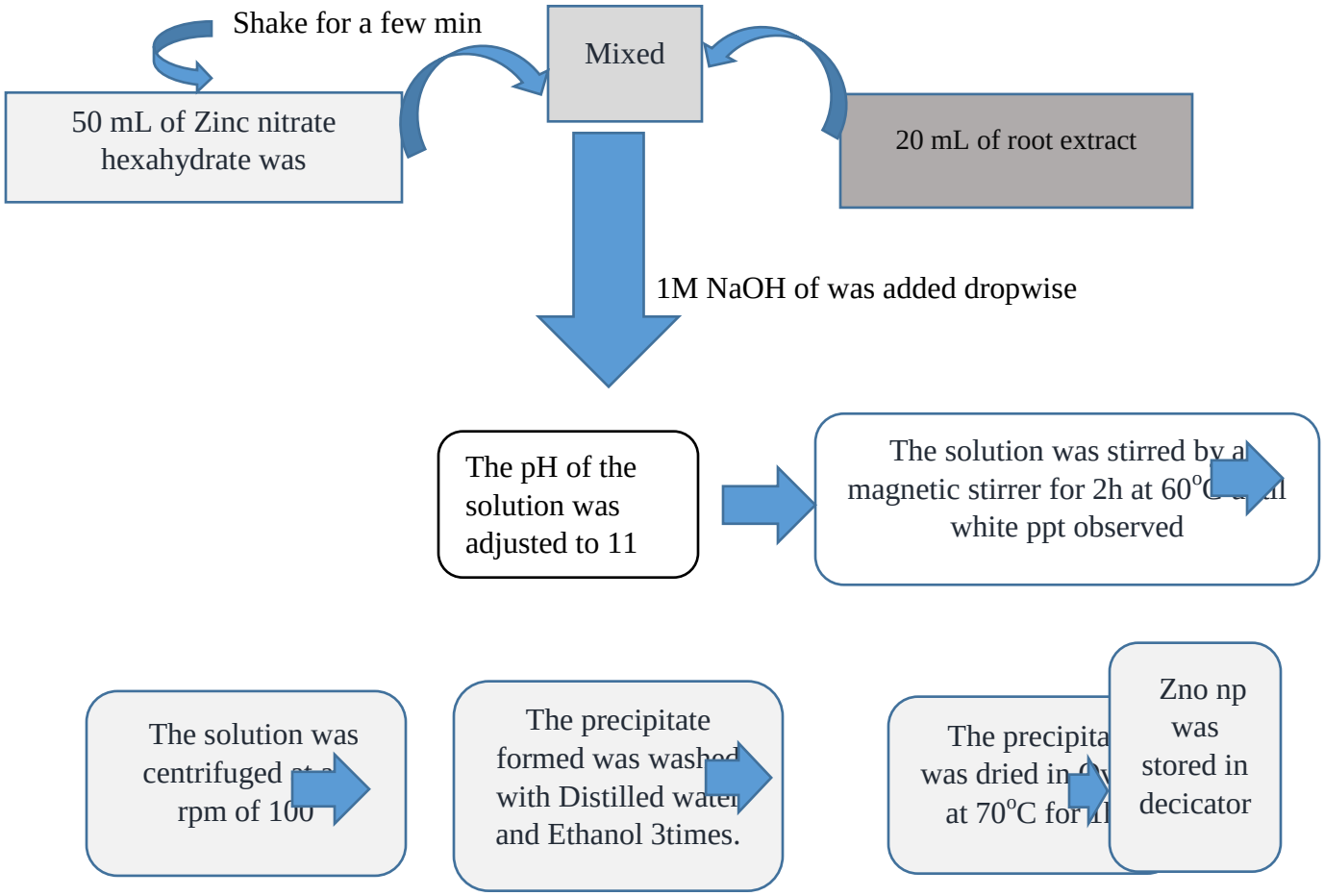

Appendix 3

The procedure of Synthesis of Iron doped ZnO nanoparticle by using ginger root extract

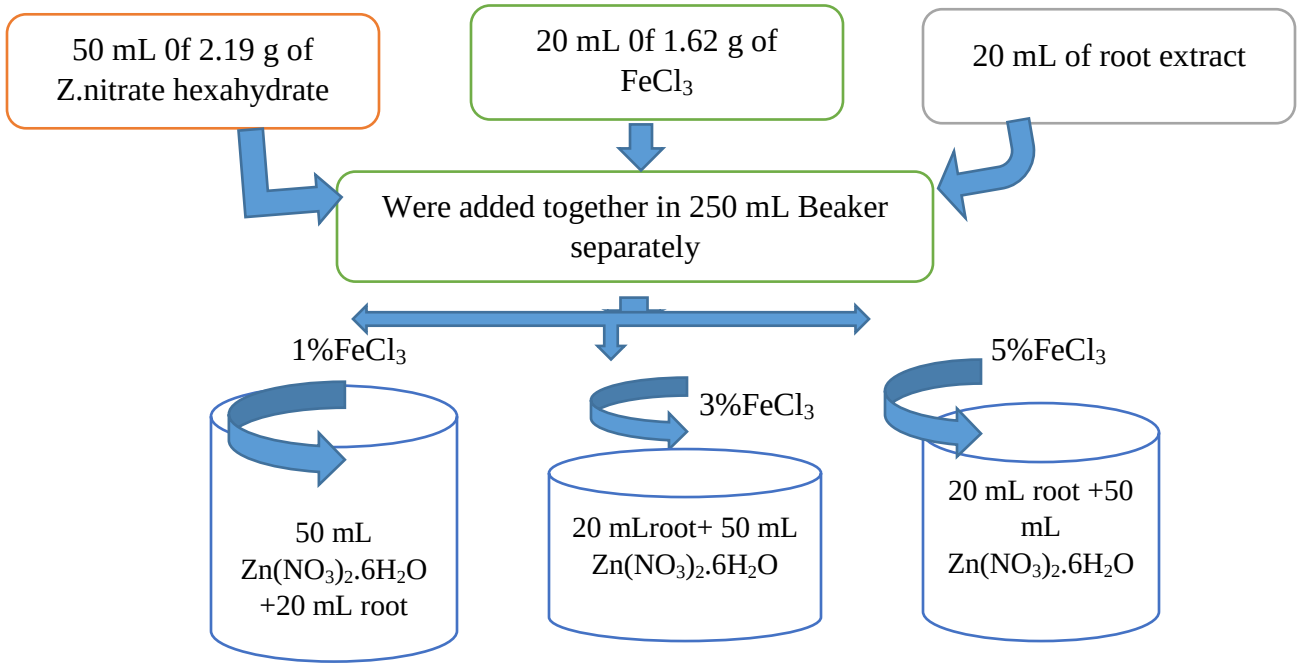

Their pH was adjusted to 11

Sample 1: $Zn_{0.99}Fe_{0.01}O$

Sample 2: $Zn_{0.97}Fe_{0.03}O$

Sample 3: $Zn_{0.95}Fe_{0.05}O$

The solution were stirred at 70^{o}Cfor 2h.

The precipitate formed was centrifuged at rpm

The precipitate was washed with water the precipitate was washed

The product was dried in an oven at 70^{o}c for 1h

Appendix4

Antibacterial assay:

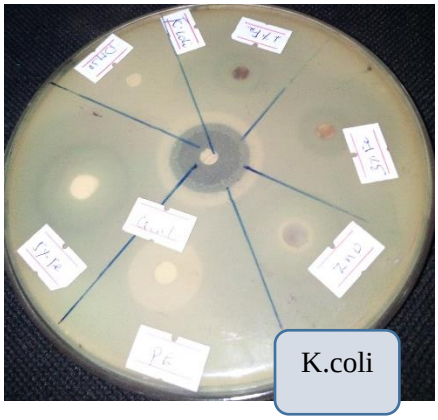

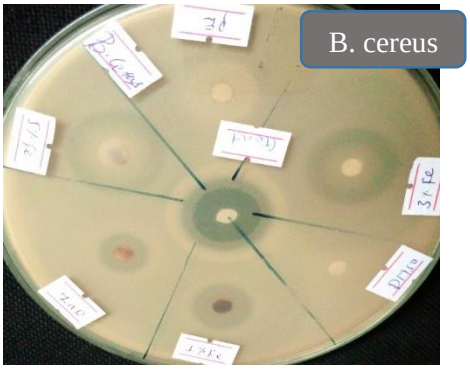

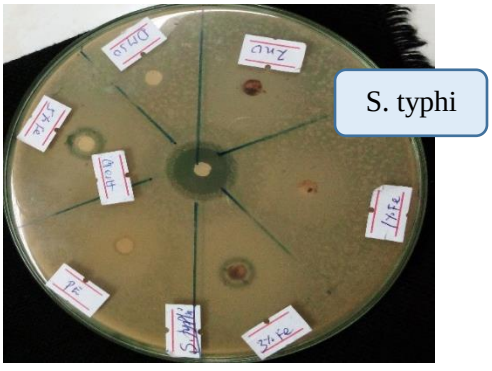

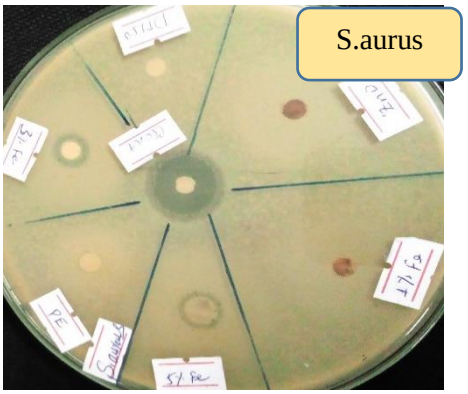

Appendix 5

Sample of Ginger Zingibber officianale from Jimma

Sample of Z.officianale that was purchased

Appendix 6

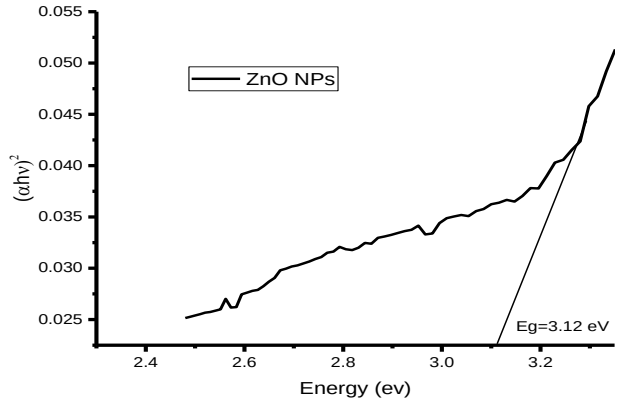

A) Energy bandgap of ZnO Nps

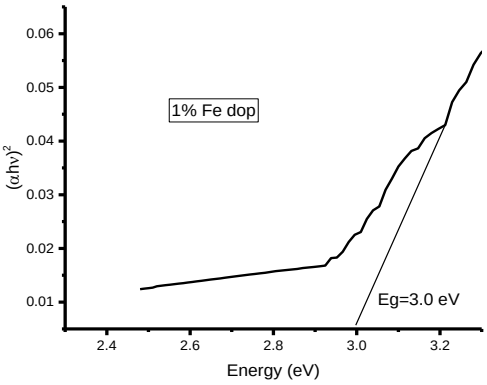

B) Energy bandgap of 1%Fe-ZnO NCs

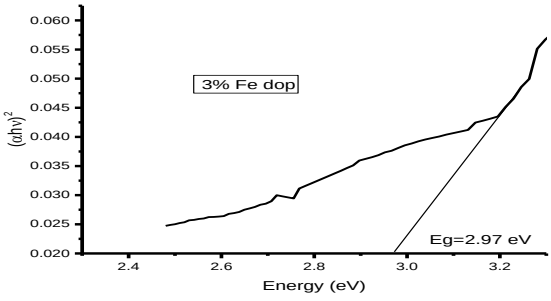

C) Energy band gap of 3% Fe-ZnO NC

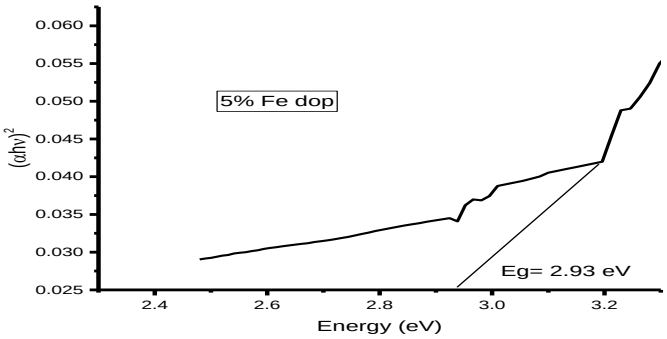

D) Energy band gap of 5% Fe-ZnO NC